UNIVERSITAT DE BARCELONA

Final Degree Project

Biomedical Engineering Degree

Self-powered system based on Microbial Fuel Cells

Barcelona, 14th June of 2021

Author: Helena Riesco Domingo

Director and tutor: Pere Luis Miribel Català

Acknowledgments

It has to be mentioned that this Final Degree project has been carried out in the frame of the project "Plataformas Sensoras Inteligentes Auto-Alimentadas para la industria 4.0", PID2019-110142RB-C22/AEI/10.13039/501100011033.

Firstly, I would like to thank the tutor and director of this project, Dr. Pere Luis Miribel for helping and guiding me in the process of development of this memory. During all these months he has always tried to explain us the difficult topics in the most understandable and less overwhelming way. I think I would not have been able to understand the concepts involved in it if it was not for his patience.

Secondly, I would like to thank my colleague Maria Penon who has also worked hard several months in this topic. We have spent many hours talking about our respective projects, and I think the process would not have been the same if I had not had her as a company.

Finally, I want to thank my family and friends, specially my mother, for always supporting me even on my worst days and sometimes believing in me more than I could myself.

Abstract

The deployment of traditional energy sources and, thus, the need for alternative options is now a reality. Although many substitutes can be considered, the development of Microbial Fuel Cells (MFCs), which take advantage of the bacteria's capacity of generating energy from the biomass, presents many opportunities. With their use, traditional batteries could be replaced and self-powered systems, which are be able to harvest, store and manage their own energy, could be created.

Additionally, as the awareness on the impacts of environment pollution is increasing over the years, the monitoring of important soil characteristics such as pH and temperature supposes a great tool to prevent contamination from happening and affecting human's health.

This project in framed in the Final Degree project of the Biomedical Engineering degree and presents an approach to develop a self-powered system based on Microbial Fuel Cells for the monitoring of soil's pH and temperature.

To do so, the simulation software *LTSpice* has been used and modelling has been performed to mimic the electrical characteristics of an MFC. Additionally, a commercial DCDC converter has been analysed and the values of its different components have been changed in order to study its performance. Then, a pH and a temperature sensor have been modelled and the needs in terms of power and voltage have been obtained.

Finally, the whole system has been combined with the MFC acting as an energy provider, the DCDC converter as the Power Management Unit (PMU) to regulate the outputs and the sensors to obtain measures from the environment.

Keywords: *Microbial Fuel Cells – Soil characterization – Self-Powered Systems – Modelling – Energy Management*

Index

1. Introduction

The World Health Organization (WHO) defines the concept of health in its constitution [1] as not only the absence of illness but as the complete state of well-being.

However, although the definition may be simple, there are multiple and diverse factors affecting it. Precisely, our natural environment plays a key role in the health of the population. There are human health hazards such as the air pollution, the presence of heavy metals or the climate change.
In addition, the conditions in which we keep our environment can not only damage our health, but rather enhance it. [2]

One clear example of the effect the environment quality can have on human's health is soil. Soil has great effects on humans' well-being which can either be direct or indirect. Many of the nutrients present in the food we consume are passed through soil. However, other substances which can arise health concerns can also be present. These substances include heavy metals and metalloids such as lead, arsenic, cadmium and mercury, among others, which not only are dangerous for humans but can also affect the soil's biota [3]. Presence of these heavy metals have been found in leafy vegetables, grains, and other crops in different concentrations around the world.

The health risks associated with the consumption of these metals include lung damage, kidney damage, endocrine disruption, adverse impact on the central nervous system and the circulatory system and multi-organ dysfunction, among others.

Because of the effects that have been found, efforts are being made and more investigation is being performed to understand the mechanisms of contamination in order to prevent it from occurring.

In terms of monitoring, one of the parameters that can be easily monitored, and which is an important indicator of soil's health is the pH. pH is a function of the number of free hydrogen ions which are present in a substance. In this sense, it is a measure of how alkaline or acid is a medium and it is measured in terms of a scale which ranges from 0, the most acidic, to 14, being this value the correspondent to the more alkaline measurement [4].

It has been found that soil pH not only affects crop yields, suitability, plant nutrient availability and the micro-organisms activity [5] but also influences the deposition of heavy metals as metal deposition has found to be low when pH is around 6.5 to 7 [6]. In general, the solubility of most heavy metals increases with the acidification of soil, this is with the decrease in the pH [7].

In addition, soil pH can also be affected by other physical parameters such as temperature as it is known that soil temperatures between 25 ºC and 39 ºC increase the acid denaturation and thus increase the pH [8].

Because of this relationship and because providing ways of improving the health of humans not only includes the activities developed inside the hospital or the products that can be offered to them but also other developments which ensure the quality of life, the improvement of ways to monitor

the pH and temperature of soil for agricultural purposes takes relevance in the Biomedical Engineering field.

Despite this, because the instrumentation needed for the monitoring of these parameters needs from energy supply, additional resources have to be considered. Traditional sources of energy that could be used include alkaline or lithium batteries. However, and because the awareness about environment damage has increased considerably in the last years, other alternatives much "greener" and less harmful for the environment are being considered.

Among these, renewable energies such as wind or solar energy have been developed and successfully applied in many places of the world. However, the energy output as well as the initial costs and efficiency are only some of the limitations which make these sources less considered than the traditional ones.

In this context, Microbial Fuel Cells (MFCs) such as the MudWatt™ offer the opportunity to take advantage of the biological energy created by microorganisms and transform it to electrical energy via the use of the electrochemical fuel cell principle. This energy can not only be stored but also be used to supply energy to the energy conversion system, making it more efficient.

On the other hand, with the increased necessity of obtaining energy from alternative sources and storing it, self-powered systems should be introduced. Self-powered systems are units which consist in different components each destined for a different task, there can be an energy harvesting unit, a data processor module, a sensor, or an energy storing unit. What it should be noted is that the main application of these systems is the obtention of energy from its environment and the posterior storage to power sensors or other electrical circuits [9]. Many examples of the use of these systems can be found in literature in which the energy sources are investigated [10], the powering of portable and wearable self-powered systems is analyzed [11] and the energy harvesting for this kind of systems is investigated [12].

Taking advantage of MFCs, a self-powered system could be developed in which energy is retrieved from microbial activity in the soil in order to fuel a sensing electronic in order to measure and control the soil pH and temperature.

Thus, this Final Degree project presents the design and simulation of a self-powered system fueled by Microbial Fuel Cells.

1.1. Objectives

Related with the concepts explained above and considering the guidelines for the Final Degree project the objectives of this project are divided in the different categories.

1.1.1. Self-powered system

As a first conception of the project, the objectives related with the development of the system itself include: understanding MFCs energy production mechanisms, modelling of MFC in an electric simulation environment, being able to obtain significant results, studying the electrical characteristics of the circuit, managing the energy provided by the MFC and being able to dimension the instrumentation used in terms of power supply.

In summary, the main objective of the project is to design and simulate an electric circuit which is able to mimic the characteristics of a MFC and successfully extract energy from it in order to supply an instrumentation.

1.1.2. Final Degree project

In terms of the final degree project and presentation of it, the main objectives include planning and developing a work related to the Biomedical Engineering field, documenting all the processes, managing the time, setting realistic goals and developing a memory with the structure of an engineering project.

Figure 1. Summary of the objectives of the system and the project

1.2. Scope and Span

The conception of this project is framed in the development of the Final Degree project. Additionally, the theme of the thesis is set between the fields of Microbial Fuel Cells for energy production, Power Management electronics and instrumentation for soil characterization.

The contents of the work include all the activities aimed at fulfilling the objectives described above divided in three main parts: MFC design and simulation, choosing a PMU option and assessing it and developing a circuitry for the instrumentation part. Because the level of initial knowledge about the subject is limited, as fuel cells are not covered in the syllabus of the degree, the level of depth acquired will be limited and only superficial and simple aspects will be considered.

Because of that, the thesis aims to approximate the field and not an exhaustive analysis. For instance, only static characteristics of the microbial fuel cells are considered leaving out the dynamic ones. Also, because of time limitations, the design and implementation of a data display system has also been left out of the scope of the study.

Thus, the project will end with the data collection from the electronics associated with the instrumentation implemented.

1.3. Methodology

The structure used for this project is based on the one used in the third-year subject “Proyectos de ingeniería” taught in the Biomedical Engineering degree in the UB by professor Jordi Colomer.

To achieve the objectives defined previously, the development of the project will consist mainly in guided, non-practical, autonomous work, including reading and learning about the subject taking into consideration the indications of the tutor and also aiming to simulate the performance of the MFCs via some accessible software.

The basis of the methodology is then the progressive increase in depth and difficulty as the knowledge of the field increases. Thus, firstly the basic aspects will be analyzed increasing the difficulty as time passes. Also, components will be considered firstly individually and then the different parts will be connected. Basically, a top-bottom and bottom-up approach will be followed.

1.4. Limitations

Among the limitations encountered, there is time, which plays a key role in limiting the scope and span of this memory.

Also, there is a spatial limitation due to the restrictions originated by the COVID-19 pandemic. This situation makes it necessary to base the project completely on computer-based simulations as well as having to perform all meetings with the tutor online.

2. Background

The work presented includes different parts with various theoretical backgrounds which have to be known before combining them. Hence, the following sections describe the most significant theorical concepts behind each subject.

2.1. MFCs as energy production systems

For many years and still, fossil fuels have been and continue to be the main source of energy worldwide. However, these traditional sources such as petroleum, natural gas and coal are quantity-limited while the energetic needs continue to arise as population continues growing and demanding more and more energy. In addition, these traditional sources of energy suppose great CO2 emissions which are damaging to the environment and which have been increasing non-stop for the last 6 decades.

Therefore, the main challenge nowadays is to solve the problem of the need for energy production while reducing the amount CO2 emissions. Among the alternatives, renewable sources of energy include nuclear fission, solar energy, and biomass energy [13].

In this context, Microbial Fuel Cells (MFCs) take importance. MFCs convert the organic material into energy via the action of microbes present in the medium. Typically, in this type of fuel cells, microbes transfer the electrons to a surface generating energy in the process. Bacteria are fed off a substrate and via a bacterial metabolic pathway the electrons are transferred so that they can be used for energy production [14].

MFCs suppose a benefit in terms of energy because they allow the direct generation of energy and can be adaptable to decentralized treatment, among others. In terms of operation stability, they present a good resistance to environmental stress, they offer the possibility of monitoring and controlling in real-time and the bacteria are able to self-regenerate. Their effects on the environment are also exceptional, presenting a low carbon footprint. Finally, in the economic field, the energy is recovered, the cost of operation is low and there is the obtention of valuable products.

The single MFC consists typically of an anode, a cathode, an exchange membrane, and the electrical circuit. The bacteria are placed in the anode and while the electrons are stripped by the bacteria, they flow until reaching the cathode while producing electricity, CO2, and water.

In terms of materials, anode need to have high conductivity and good biocompatibility while presenting chemical stability, resistance to corrosion and mechanical strength and toughness. For that reason, carbon materials are predominantly used. The cathode, which must allow for the reduction reaction, is often made-up of graphite, carbon felt, carbon cloth and carbon paper [15].

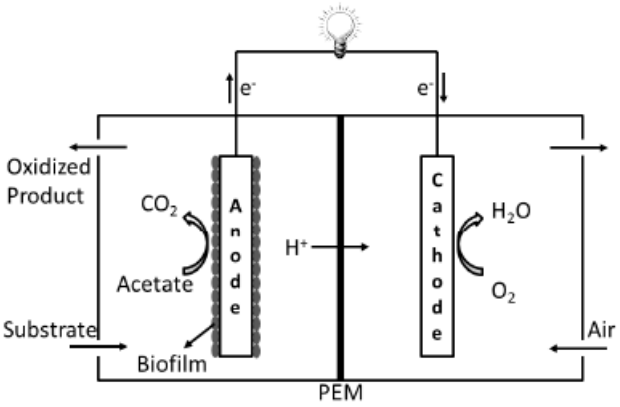

Figure 2. Typical structure of a two-chamber MFC [16]

As for the applications of MFCs different categories can be distinguished such as their use for wastewater treatment, their use in landfill, the generation of electricity via Plant-MFCs, for hydrogen production purposes and their use for powering microelectronic devices.

In this last field, MFCs have been found a great alternative to chemical battery cells and have been found to be cost-effective. In addition, the ability to work autonomously supposes a great advantage as they can be used in systems where, because of the localization for example, it is difficult to have access to replace the batteries.

To assess the electric performance of MFCs, different analytical techniques have been developed. Hence, the typical performance indicators used are the following:

- Open Circuit Voltage (OCV). It is "the maximum voltage that is obtained from a cell at infinite resistance as the OCV value does not take the voltage losses into account" [15]. This is an ideal situation as in real life the losses suppose a decay of this value.
- Current generated. The current of the fuel cell can be calculated using the Ohm's law considering the values of the working voltage and the external resistance value. It provides a vision of the rate of electron transfer.
- Power generated. The power generated in the FC can be obtained by multiplying the working voltage by the current.
- Polarization. It represents the voltage of the fuel cell in terms of the current flowing. There are two main ways of finding it: performing a sweep in the voltage using a potentiostat or varying the value of the resistance. The typical polarization curve can be divided into three main parts:
    1. OCV falls due to losses related with the activation of the reactions in each of the components of the cell
    2. There is a steady decline caused by the ohmic losses related to the electrical components of the cell
    3. At high currents, the voltage decays almost completely due to concentration polarization.

In figure 3, the typical curves obtained for both the power and the polarization of the cell can be seen. Even though the parameter used is the current density and not the current itself, the shape remains the same for both cases.

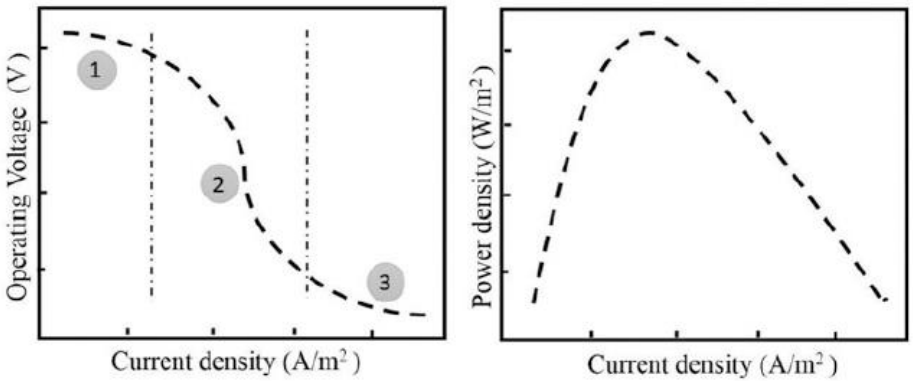

Figure 3. Typical polarization and power curves for a single MFC [15]

The typical output values in terms of voltage are around 0.2 V to 1 V. However, in order to pump-up the outputs of a single fuel cell, other configurations have been studied and it has been found, for example, that the output voltage of 4 MFCs stacked increases from 0.7 V to 2.5 V.

2.2. Power Management Unit

The Power Management Unit also commonly known as PMU is a system that ensures that the level of power provided by a given electricity at any time is in line with the load voltage needs [17]. Also, PMUs allow the storage and use of the harvested energy.

The PMU is composed of basically two blocks [16]:

- Energy Shaping block. This part has to extract the maximum power from the energy source. MPPT, power tracking to extract the best energy adapting the impedances between the source and the electronics supplied.
- Power Regulator. In this part, the maximum available power is taken and converted into the required voltage by the load. This process is done via up-conversion, rectification, down-conversion, or a combination.

PMUs take relevance in the field of MFCs when considering that the typical output voltage of a MFC is of 0.2 V – 1 V while most electronic devices require a voltage between 1.8 V to 5 V and a minimum of some mW to function properly. Because of this difference, PMUs are needed to boost the outputs of the MFC to a range that is suitable for the electronics to start-up. However, most PMUs require high start-up voltages, above 0.6 V, which is not attainable by the majority of MFCs [18]. Despite this, some can also function with lower tensions but in these cases, there is usually the need for a transformer element. Also, because MFCs are based on a biological process, non-linearity is associated and, as the substrate is consumed, the levels of voltage provided may vary.

In this sense, commercial DCDC converters are usually used. DCDC converters include a passive and an active part. The passive part is composed of inductors or capacitors while the active part is based on semiconductor technologies which have to surpass a certain voltage level to work properly. Because of the presence of these active elements, when working with DCDC converters it is important to consider the start-up voltage which is the minimum voltage at which the circuit can start operating.

2.3. Sensors

A sensor is a device that can detect a physical or chemical change in the environment and convert this detection to a signal that can be quantified such as an electric signal.

There are many types of sensors aimed at different applications such as temperature sensors, proximity sensors, infrared sensors, humidity sensors, etc.

Regarding the type of sensors included in the scope of this work, the pH sensor and the temperature sensor, many commercial options are available.

2.3.1. pH sensors

Typical pH sensors consist on a electrochemical cell composed by the measuring electrode which is usually made of Sodium Ion Selective Glass and is in contact with the solution from which the pH value is computed. The other electrode is the reference electrode which is not in contact with the medium and thus provides a reference for the measuring electrode.

The basis of the measurement is the property that states that when two liquids with different pH come into contact, an electric potential is generated. Regarding this relationship, as the pH of the solution increases the voltage generated at the measurement electrode decreases.

$$pH_{unknown} = pH_{known} + \frac{(E_{known} - E_{unknown})F}{RTln(10)}$$

Equation 1. Relationship between the pH and the voltage of a pH sensor [19]

Where pH are the pH values for each solution, E are the electric potentials, F is the Faraday constant, R is the universal gas constant and T is the temperature (K) [19].

The typical pH sensor electric circuit includes an amplifier, an Analog-to-Digital converter, a microcontroller and the display, as it can be seen in the following picture [20]. It has to be considered that the internal resistance of the sensor is in the order of the MΩ.

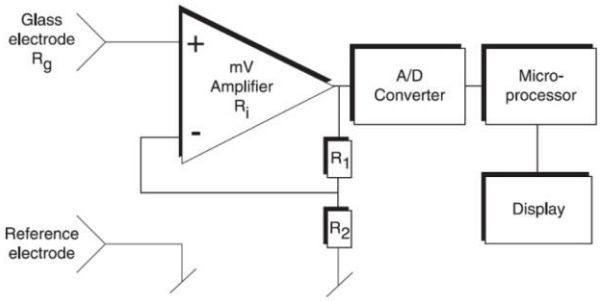

Figure 4. Electrical configuration of a pH sensor [19]

Some examples of pH sensors can be found such as the ones provided by *Metler Toledo* [21] which ensure rapid and accurate results as well as different options for table measurement for instance. On the other hand, other examples can also be found in webpages such as *mrc laboratory instruments* [22] offering pH sensors ranging from 0 to 14 in the pH scale with a resolution of 0.001 pH units and a voltage resolution of 0.1 mV. Additionally, some of these sensors also include a temperature sensor for temperature compensation.

2.3.2. Temperature sensors

For the temperature sensors, many options are available offering different characteristics. There can be found IC sensors, thermistors, RTDs and thermocouples. Of all of these, the option which offers the best accuracy and linearity are RTDs (Resistance Temperature Detectors). RTDs are sensors which are made up of a metal which has a very known temperature – resistance relation. [23]

As for examples of this type of sensors, several can be found. Only from *Texas Instruments* the lmt84 can be found, which has a low, 1.5 V, operation with high accuracy, 0.4 ºC; also the lmt85, with a 1.8 V operation and the same accuracy as the previous; and the lmt88 and lmt89, with the same operation point, 2.4 V.

On the other hand, in the *Analog Devices* catalogue [24], 33 digital temperature sensors can be also found. These vary in the number of channels, 1 to 20, the temperature sensor interface (diode, internal temperature sensor, RTD, thermistor or thermocouple) and the supply values, with minimum values ranging from 2.65 V to 4.5 V and maximum values ranging from 3.3 V to 7 V. The prices also vary considerably among these.

3. Market analysis

3.1. MFC market

Consulting the *Web of Science* [25] webpage taking advantage of the UB credentials, the statistics related to the MFC field could be investigated.

The term Microbial Fuel Cells was introduced as the search input and the result analysis option was selected. In total, from the last 25 years, 14412 records were found related to the topic.

In relation to the research areas, the biggest research area was their use as energy fuels, with 8180 publications, followed by the area of engineering, biotechnology applications and environmental sciences, all three around the 7000 publications each.

Analyzing the results based on the publication years, it can be noted a clear increase in the interest for this topic, while in 1997 only 15 papers were published, in 2018 the number of papers published was of 1519.

Also, more than a 50% of the total publications come from both China and the United States, and only 395 of the total references are Spanish. This could be an advantage because there is more field to develop this topic in the country but also a disadvantage for research groups because not much funding may be found and the collaboration with near groups will also be more difficult.

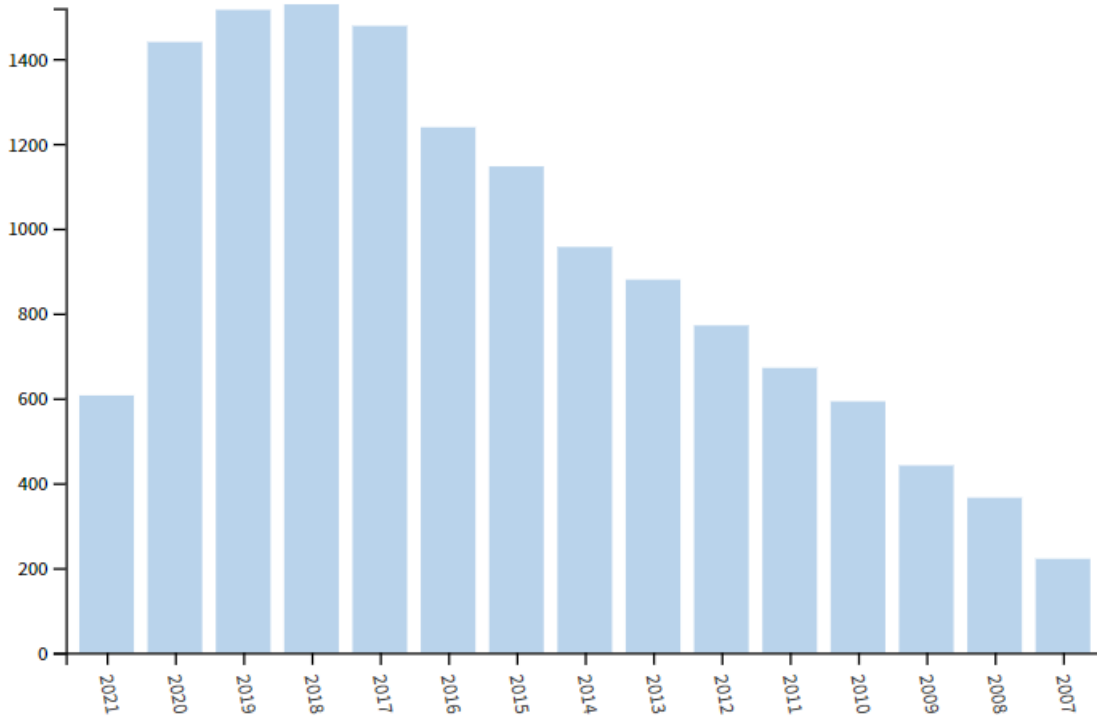

Figure 5. Evolution of the amount of publications per year 1997-2021 [25]

The market has been segmented into four different categories: type, application, end-user and region [26]. In the type category, the mediator and non-mediator options can be found; for the

application field, four applications are distinguished including power generation, wastewater treatment, biosensor and others. Regarding the end-user, five sectors can be distinguished: agriculture, food & beverage, healthcare, government & municipals and others. Finally, the different regions include North America, Europe, Asia-Pacific, Middle East and Africa and South America.

The main companies governing the market are:

- Pilus Energy LLC (US)
- Fluence Corporation Limited (US)
- Triqua International BV (The Netherlands)
- Electrochem Solutions and Emefcy Ltd (US)
- MICROrganic Technologies Inc. (US)
- Prongineer R&D Ltd (Canada)
- Vinpro Technologies (India)
- Sainergy Tech (US)

3.2. Future perspectives of the market

As the consumption of non-green combustibles continues, the sources will continue to deplete and other options will have to be investigated. It is predicted that the MFC market will grow considerably due to the investment of companies and governments.

In terms of future prospections, while in 2018 the market size was of USD 9.6 Million, it is expected that by 2026 it will reach the USD 19.5 million [27].

4. Conception engineering

Because one of the main objective of the system to develop is to be able to use the fuel cell to power a given electric instrumentation different parts and options for each of the parts have to be studied and a decision on the structure has to be made taking into account the characteristics of each of the components.

4.1. Study of solutions

4.1.1. Simulation software

Because the project experimental part is based on simulations, an adequate simulation software needs to be chosen.

In terms of electronic circuit simulators, there are several commercial options available, some of them are Altium Designer, Circuit Simulator, Micro-Cap, CircuitWizard, Virtual Breadboard, Pspice, LTSpice, iCircuit, PSIM or QUCS.

The software used has to allow for the easy and accurate representation of the electric models and the obtention of data has to be relatively fast.

4.1.2. Structure of the system

In order to function properly and as it has been previously introduced, the system has three main parts which are:

- **The MFC** itself which is the basis of the work and will provide the energy to fuel the system. This energy has a given value which needs to be assessed before considering any of the other parts.
- **The Power Management Unit (PMU)** which will take the voltage level provided by the fuel cell as an input and will return regulated tensions and currents according to the needs of the following instrumentation.
- **The instrumentation** associated which will be powered by the system and will be used to gather the information needed from the environment.

Thus, the structure used will be the following:

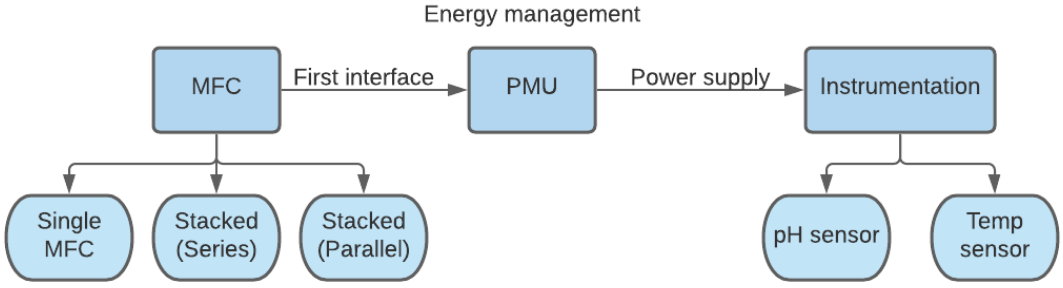

Figure 6. Structure of the self-powered system

4.1.2.1. MFC study

In terms of configurations available for the MFC, there are mainly three options depending on the application and the range of energy supply needed:

- **Single MFC**. Single fuel cells configurations give outputs typically between 0.2 V and 1 V.
- **Stacked in series.** Here, the voltage provided by the system can be increased proportionally to the number of fuel cells stacked. This configuration may be used for applications in which a large output voltage is needed. Some of the problems associated with this type of configuration include mismatches which can result in one MFC absorbing the energy provided by the rest and thus being detrimental to the final goal of producing energy.
- **Stacked in parallel.** In this case, the current provided increases proportionally to the number of fuel cells stacked. This configuration might be useful for applications in which large current quantities are needed.
- **Combination of stacking in series and parallel.** Finally, the combination of the advantages of both stacking options can be done by stacking the FCs both in series and in parallel.

4.1.2.2. Power Management Unit possible solution

The main problem of the use of MFCs to provide energy is the often mismatched provided and needed energy levels. For this reason, this unit has to be able to provide the necessary amount of energy at the output taking as the input the energy of the fuel cell.

The complexity of the PMU will depend greatly on the number of fuel cells present in the system. However, there are already commercial options available which condense all the characteristics needed. Below some options, are presented [28]:

PMU	Start-up voltage (mV)	Operating point (mV)	Regulated output?
BQ255	330	80	Yes
LTC3105	250	225	Yes
LTC3108	20	20	Yes
S-882Z	300	300	Yes
ECT310	20	20	No
SPV 1040	300	300	No

Table 1. Different PMU options available

4.1.2.3. Instrumentation possible solution

The pH sensor signal, which would be obtained from the measurement electrode, can be emulated using a voltage source which changes over time. However, because the typical sensors have a high output impedance, in the order of the GΩ, a high precision operational amplifier which buffers the output is needed. The input bias current of said amplifier needs to be low in order to reduce the offset.

The amplifier selection can be difficult as there may be considerable demands. In this sense, some aspects to consider are the need for ultra-low power, low noise associated, zero drift, rail to rail input and output, solid thermal stability, and repeatability [29].

Because there is a bias current flowing through the electrode resistance, the low input current amplifier reduces the voltage error associated. Following this, if there is a typical value of input bias current of 200 fA, the corresponding offset error would be of 0.2 mV which considering the pH ranges managed is equal to an error of 0.0037 pH. If, for example, a maximum value of 1 pA input bias current was obtained, this would only correspond to a variation of 1 mV, which in terms of pH is only 0.0185 [30].

In this line, the temperature sensor can be emulated using the same approach but changing the directives applied.

4.2. Proposed solutions

4.2.1. Software proposed solution

In terms of software, the selected option is **LTSpice** as it is the one that has been mostly used during the degree.

LTSpice allows for the simulation of models, the capture of schematics and the viewing of waveforms. It also includes many components in its libraries such as the ones from Analog Devices.

4.2.2. MFC proposed solution

Considering that the this is an initial study on the field, the Single MFC configuration as well as the series-stacked and parallel-stacked will be studied to note their electric performance. However, only the **Single MFC** configuration will be considered to connect it to the rest of the system.

The reason for this election is that, although stacked options may provide higher outputs in terms of voltage and/or current, the most research has been performed for the single option and it will be easier to obtain references for this case.

4.2.3. PMU proposed solution

The solution chosen is the LTC3108 DC/DC converter as it is the only one, together with the ECT310, that has a start-up voltage below 250 mV. In addition, in comparison with the ECT310, it has a regulated output which is useful because although the source may get uncontrolled and the load may change, the output voltage remains tightly controlled.

Additionally, the LTC3108 is already designed for energy harvesting applications. The circuit can be seen in the following figure:

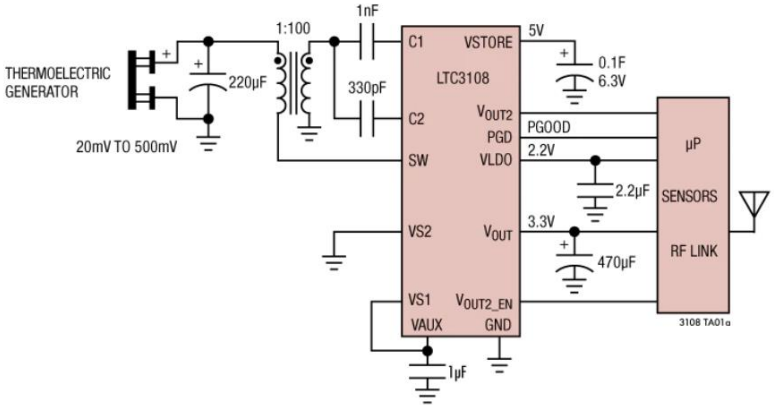

Figure 7. Structure of the LTC3108 DCDC converter [31]

Regarding its functioning, it uses a MOSFET switch using a step-up transformer and a small coupling capacitor [31]. The frequency of oscillation, determined by the inductance of the transformer, is between the 20kHz and 200kHz.

The voltage produced in the transformer is boosted and rectified using a pump capacitor.

As soon as the Vaux terminal reaches the 2.3 V, the VLDO achieves a value of 2.2V. The current of the LDO node is limited to a value of 4 mA.

Regarding the STORE node, the capacitor can take values from the mF to the F, and it can charge up to 5.25 V.

The system allows for the output of 4 voltage levels (2.35 V, 3.3 V, 4.1 V and 5 V) depending on to which pins are VS2 and VS1 connected. For an output voltage of 3.3 V, VS1 needs to be connected to VAUX while VS2 must be connected to ground.

4.2.4. Instrumentation proposed solution

Because of the characteristics needed for the amplifier, the ADA4661-2 has been selected for this study.

This amplifier is optimized for low power and wide operating supply voltage range applications. One of its applications includes the use in high impedance sensor interfaces.

Among its characteristics it can be found that the offset voltage is low (150 µV max) and the input bias current is also low (15 pA max), these two characteristics are important, as it has been stated before, because with them, the effects of the offset on the measurement is reduced.

Also, the input resistance is very high, above the 10 GΩ, which is useful to prevent the current drawn to the amplifier.

Additionally, the single-supply operation moves between the 3 V to the 18 V and thus is suitable for the combination with the PMU selected, which has a regulated output of 3.3 V.

Regarding the open-loop gain, which ideally should be infinite as the main function of the op-amp is to amplify the signal, has a typical value of 130 dB, corresponding to a gain of 3e6 V/V.

Concerning the bandwidth, which ideally should be infinite to ensure the correct functioning in every frequency, it is high. The Gain-Bandwidth product is of 4 MHz.

Finally, the output resistance is wanted to be as low as possible, ideally 0, as it will be in series with the load and, consequently, reducing the voltage supplied to the load which is the opposite of the desired situation. In this case, its value is of 0.2 Ω [32].

To sum up, the characteristics that have been considered to choose the ADA4661-2 amplifier for this application can be seen in the table below:

Characteristic	Value	Units
Offset Voltage	150	μV
Input Bias Current	15	pA
Input resistance	>10	Ω
Single supply operation	3	V
Open-loop Gain	130	dB
Gain-Bandwidth product	4	MHz
Output resistance	0.2	Ω

Table 2. ADA4661-2 characteristics

5. Detail engineering

In order to obtain the electrical characteristics, some simulations have been performed. In the following pages, the different steps taken to fulfil the simulations to characterize the MFC, PMU and instrumentation are detailed.

5.1. MFC characterization and simulation

5.1.1. Single MFC configuration

As a first step, the fuel cell to characterize had to be identified and simulated. As fuel cells will have different electrical characteristics depending on the type, a reference for the microbial fuel cell had to be found.

One of the main features that has to be considered for this characterization is the polarization curve which has already been described in the introduction. In it, the current supplied by the cell is located in the x-axis while the voltage supplied is represented in the y-axis. In this way, for each current there is a voltage associated.

Different examples of polarization curves were examined and as a reference, the one in the thesis of Nicolas Degrenne was used as a guide [28]. In this case, and having only one MFC, the open circuit voltage was found to be approximately 550 mV.
The first step in the study was to obtain different reference points of the curve. Because if no spreadsheet is available it is difficult to calculate these values by eye, the tool *WebPlotDigitizer* was used. This tool allows to take the image of a graph and, setting the axis limits, be able to calibrate the values. Once calibration is done, the different points of interest can be selected.
In total, 20 points were taken ranging between 546 mV (open circuit voltage) and 23 mV (corresponding to 6.37 mA).

After that, the fuel cell was simulated using the *LTSpice* software. This model includes different components which include a voltage source controlled by *E1, Vsense* which acts as an amperemeter, a fixed-value resistor which will allow the control of the tension in the *E1* voltage source as a function of the voltage drop in the resistor.

This control of the value given by the voltage source was programmed using functions from the *Analog Behavioural model*. This modality allows to model the behaviour of components from a macroscopic point of view rather than from a microscopic one. This is extremely useful in the black-box modelling of complex systems.

Taking advantage of this LTSpice feature, the *table* function was used and applying the Ohms law, the value of the voltage was controlled, putting as a first argument the voltage wanted in the x-axis and as a second argument the value of the voltage obtained from multiplying the desired wanted (the one in the x-axis of the reference) by the resistor value:

$$V_{inserted} = I_{Vsense} \cdot R_1$$

Equation 2. Ohms' law applied to the FC

Then, to control and simulate the presence of a load, a set of switches was implemented. Because the initial resistance is in the order of GΩ, there will be no current drawn and thus the configuration will be in open circuit. However, this set of switches can be programmed to close at determined times by the imposition of a voltage threshold activated transition. This transition is run by a model called MFC, which has a threshold voltage associated of 0.5 V. Thanks to this, and because each switch has a resistance associated and is connected in parallel with the rest of switches, every time that one switch closes, the total resistance decreases which will be demanding more current to the fuel cell and thus simulating the presence of a load.

In total, 13 switches were implemented, each one closing every 0.5 milliseconds. The implementation of more switches allows a smoother transition between values rather than a more scaled.

Finally, in terms of design, and in order to make the schematics clearer the last step was to create a *LTSpice* symbol for the switches and another one for the complete fuel cell itself.

The schematic of the model used for a single fuel cell was the following:

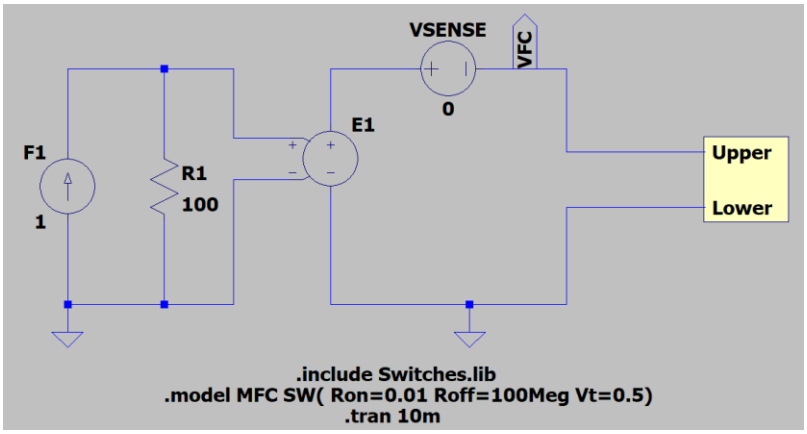

Figure 8. Schematic of the Single MFC configuration

5.1.2. Stacked fuel cells

Having a basic knowledge about the electrical characteristics of the single MFC, different stacked configurations were studied. Stacked configurations are interesting for multiple applications in which either the voltage or the current needs are above the ones provided by a single fuel cell.

5.1.2.1. Series configuration

For applications in which there is a need for higher voltages, above the 546 mV offered by the single configuration, a series configuration can be considered.

In order to study this effect, first an additional voltage source was added connected in series to the previous one. Because we are considering that all fuel cells are equal, the same table of values was used to program the voltage deliver. In the case of series configuration, the voltage supplied increases proportionally to the number of fuel cells included.

$$V_{supply} = V_{OC} \cdot N_{fuel_{cells}} = 0.55\ V \cdot N_{fuel_{cells}}$$

Equation 3. Relation between the FC voltage and the number of FCs

Because the voltage is proportional to the number of fuel cells, when the voltage increases, for the same value of current, the power increases proportionally. Because of this, the power value doubled with the addition of an extra fuel cell.

For the design using *LTSpice,* each fuel cell stacked was simulated using a voltage source, the positive and negative inputs of each one were connected, adding in this way the voltages supplied by both of them. Finally, the schematic used was the one in figure 9.

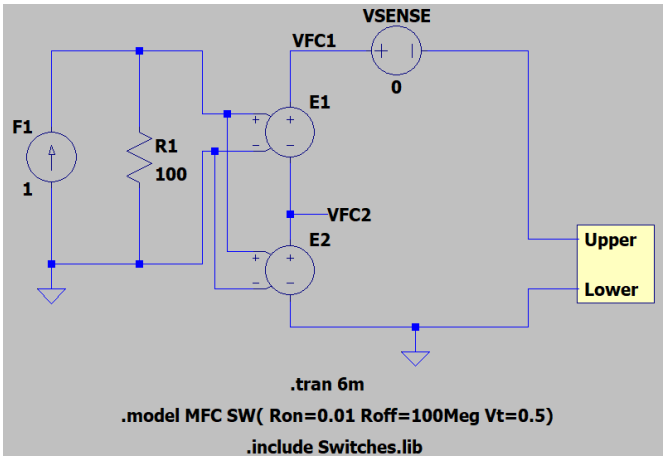

Figure 9. Schematic for the two MFCs stacked in series

5.1.2.2. Parallel configuration

The next step was to perform the same simulation but this time building a parallel configuration. For this new configuration, the values used for each of the voltage sources was the same as before.

With this, the currents obtained were proportional to the number of fuel cells displayed. On the other hand, and conversely to what happened with serial connection, the voltage will remain the same for all options.

$$I_{supply} = I_{SC} \cdot N_{fuel_{cells}} = 6.3\ mA \cdot N_{fuel_{cells}}$$

Equation 4. Relation between the FC voltage and the number of FCs

In terms of power, because of the relationship stated above, the power also remains proportional to the number of fuel cells stacked.

In this case, the voltage sources were kept unconnected. However, the outputs of each of the cells were connected to a common node. The resistances were added to be able to measure the currents in each of the branches.

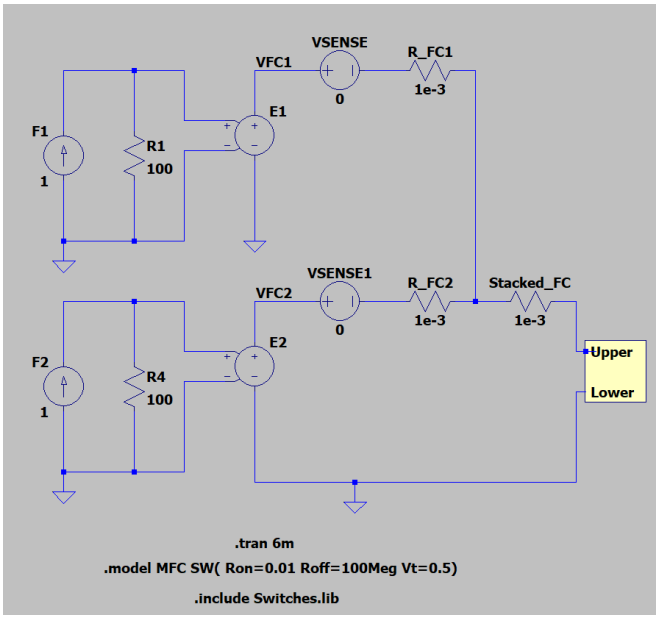

Figure 10. Schematic for parallel configuration of 2 stacked fuel cells

5.2. Power Management Unit

Once the fuel cell, which will act as a voltage source, was electrically characterized thanks to the use of the simulation tool, the power management unit was also electrically simulated and analyzed to ensure that it was suitable to combine the fuel cell and the instrumentation that will be fed from it. As it has been mentioned before, the LTC3108 DCDC converter from *AnalogDevices* was used. In this sense, the output of the microbial fuel cell was introduced as an input to the DCDC converter.

Because this option has a start-up voltage as low as 20 mV, there were no problems in the range.

After connecting the fuel cell to the DCDC converter, a particular working point is set, which will be one of the ones displayed in the polarization curve. In this case, the working point was corresponding to a voltage of approximately 70 mV and 5.5 mA.

Despite this, it was observed that if the fuel cell was used without the switches the system was not able to start working. This was because not enough levels of current were achieved and thus the MFC was left with the switches.

Having connected the fuel cell to the entrance of the LTC3108, a load was added to the output to simulate the instrumentation that will be placed after. For that purpose, a resistance with an initial value of 1 GΩ was added to output node.

After, the value of the resistance was varied using the *step param* directive and ranging the values of the resistor as needed. Also, the simulation was run using a *transient* directive.

To end up this part, diferent load capacitor values were used to see how it stabilized the circuit as

The final schematic used for this part was the following:

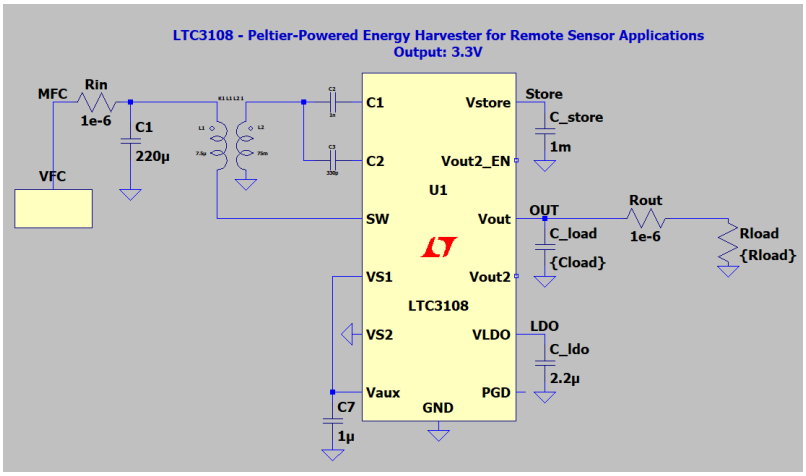

Figure 11. Fuel cell connected to the DCDC converter

5.3. Instrumentation

In this final section, the main objective was to determine the levels of energy supply needed to maintain a correct and stable function of the instrumentation. For this purpose, the instrumentation was assessed individually first as it has to be correctly dimensioned and, to do so, the correct values of the resistors and the correct configuration of the op-amp has to be selected.

5.3.1. pH sensor

In the first instrumentation type, a pH sensor was emulated. To do it, the article [33] was used as a reference.

Typically, the real pH sensor has a reference electrode which value does not change with the variation of hydrogen ion concentration. In addition, a measuring electrode which will give the pH value is put into contact with the solution of interest and, to correct changes due to temperature, a temperature sensor is also added [34].

In terms of the measurement itself, ideally, the voltage has to decrease with the pH, specifically 59.16 mV per pH unit. To emulate this increase of pH, the voltage source was programmed to supply voltage between the 50 mV and the 450 mV using a PWL directive. The pH was decreased every 10 seconds to obtain a constant slope. Taking into account this, it was considered a pH range from the unit 1 to the 7 and as soil usually takes up more metal with decreased pH levels.

To mount the circuit, the output of the voltage source was connected to the input of the ADA4661-2 amplifier with a non-inverting configuration. The amplifier power supply was connected to a voltage source providing a stable signal of 3.3V to imitate the voltage level that would be received from the DCDC converter.

The gain chosen was of 1.5 to move between the 75 mV and the 675 mV. To obtain this gain, R1 was first set to 100 Ω and R2 to 200 Ω. However, it was observed that using such low values resulted in a high drawn of intensity by these resistances. For this reason, the final values used for the resistance were of 1 MΩ and 2 MΩ for R1 and R2, respectively.

A transient directive was chosen to obtain the different parameters evolution with time. The final schematic used for this option was the following:

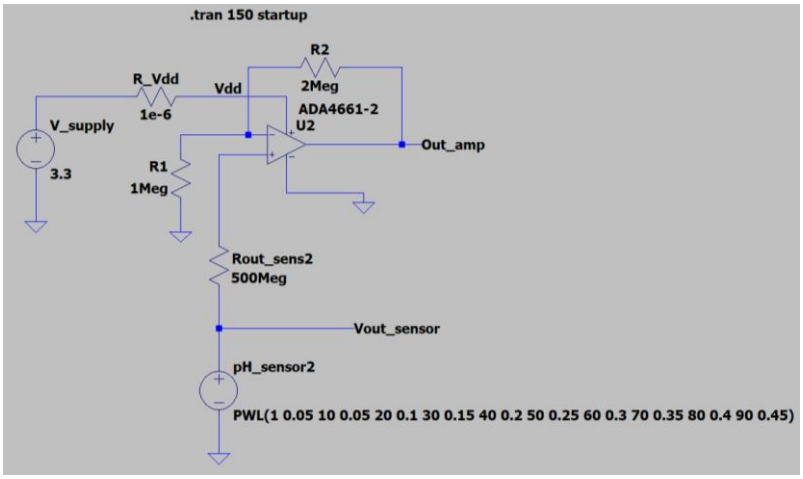

Figure 12. Schematic for the pH sensor

The typical pH sensor response is the following [19]:

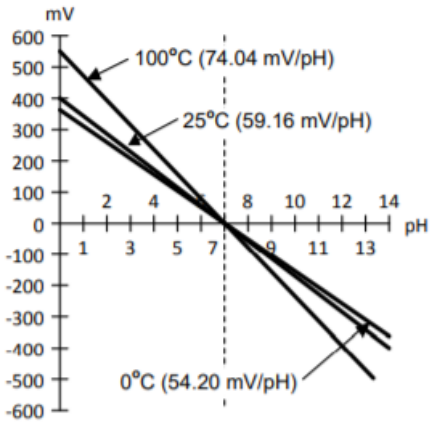

Figure 13. Typical response of the pH sensor [19]

Considering a temperature of 25 ºC as there has been considered a variation in the voltage of 59.16 mV/pH, the graph obtained for the simulation supposes an initial higher value for the pH and its decrease with time, resulting in an increase of the voltage with time. This is correct as we are

starting with a pH value of around 6.5 and decreasing it until the 0 approximately for which value it is maintained constant.

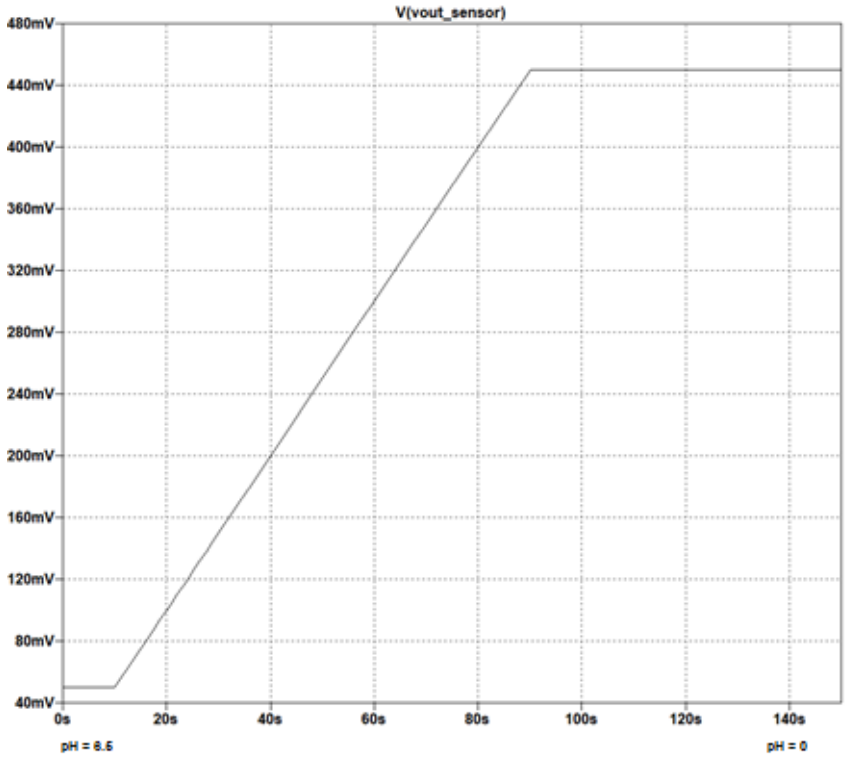

Figure 14. Response obtained from the simulated option

5.3.2. Temperature modelling for the FC

Finally, the modelling of the temperature behaviour in the FC was aimed. To do so, first, an RTD (Resistance Temperature Detector) was implemented alone and the outputs in terms of voltage and resistance were studied and compared with a reference.

To continue, the RTD was combined with the ADA4661-2 amplifier to see which levels in the output in terms of voltage were achievable.

Then, and to complete this part, the RTD was applied directly in the fuel cell model. In this way, the final part with the amplifier was not touched and the variation of the temperature was noticed directly by the fuel cell.

The formula used for the programming of the RTD resistance was the following:

$$R_{RTD} = R0 \cdot (1 + (t_{c1} \cdot T) + (t_{c2} \cdot T^2) + T_{c3} \cdot (T - 100) \cdot (T^3) \cdot (1 - u(T)))$$

Equation 5. RTD resistance variation with temperature [23]

Where:

$$t_{c1} = 3.9083e - 3$$

$$t_{c2} = -5.775e - 7$$

$$t_{c3} = -4.183e - 12$$

$$R0 = 100$$

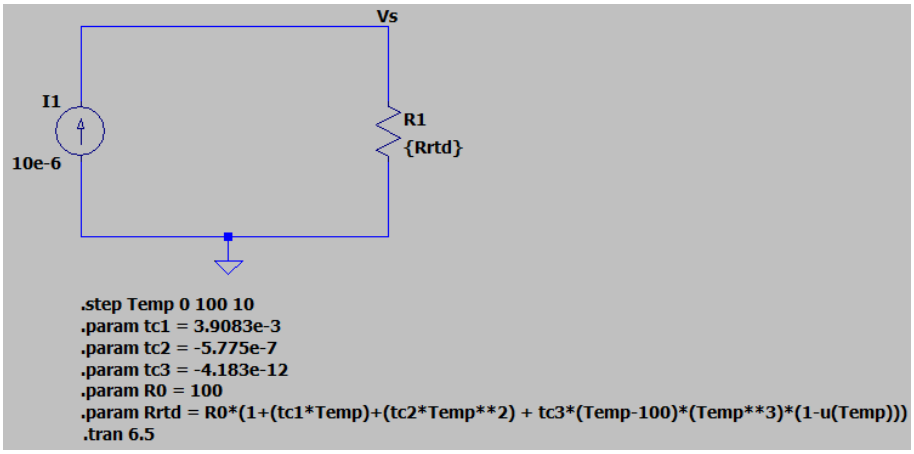

Figure 15. RTD resistance model

In figure 16, it can be seen how the resistance varies depending on the temperature applied. As the temperature increases, the resistance also increases and, as the injected current is constant and equal to 10 μA, because of Ohm's law, the voltage Vs also increases.

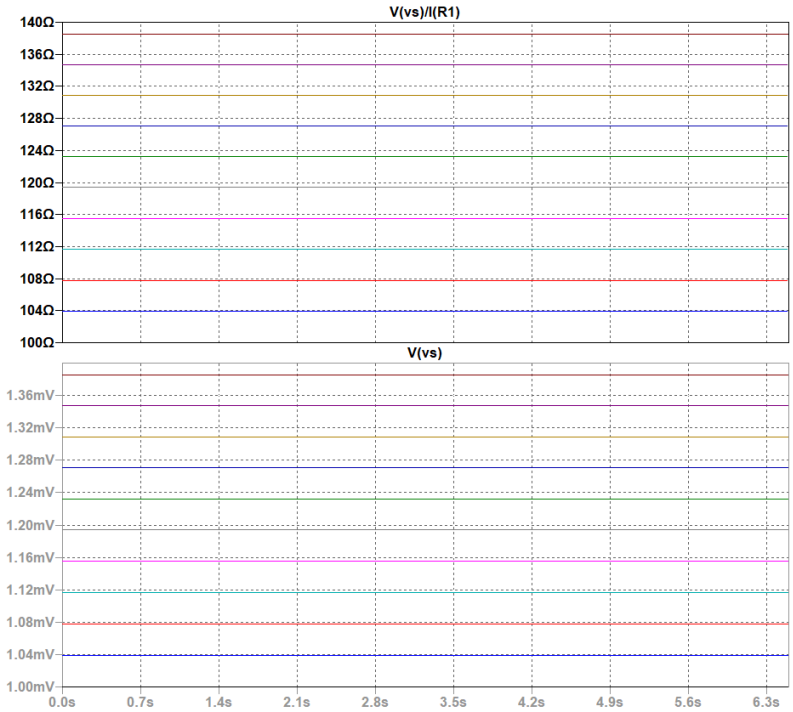

Figure 16. Dependance of the MFC resistance in terms of temperature

If these values are set in a graph with the temperature in the x-axis and the resistance in the y-axis, the graph in figure 17 is obtained which is similar to the typical response of the RTD, in figure 19. With this, the simulation of the RTD itself, without its combination with the FC or the amplifier, has been carried out successfully.

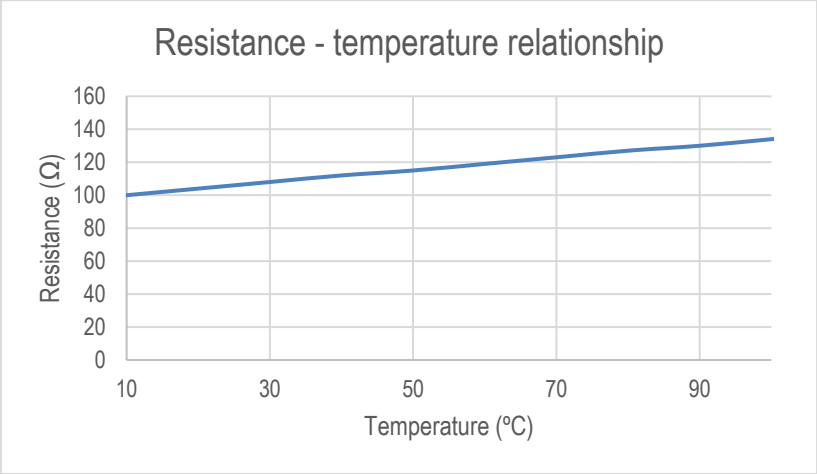

Figure 17. Relationship between the resistance and the temperature

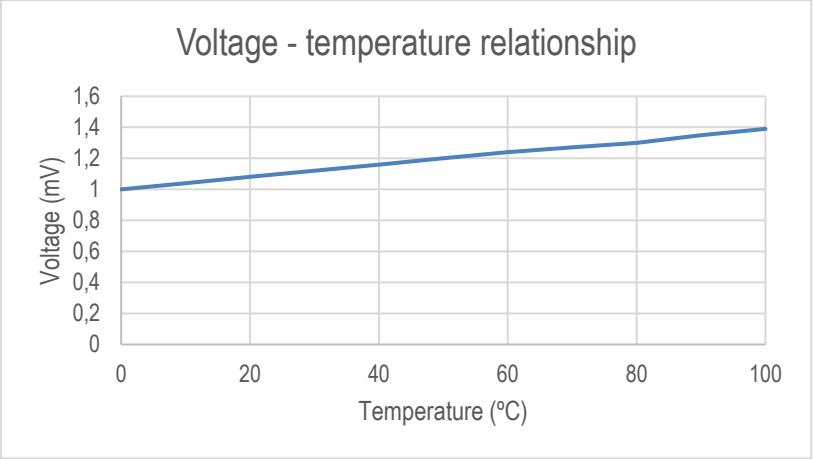

Figure 18. Relationship between the voltage and the temperature

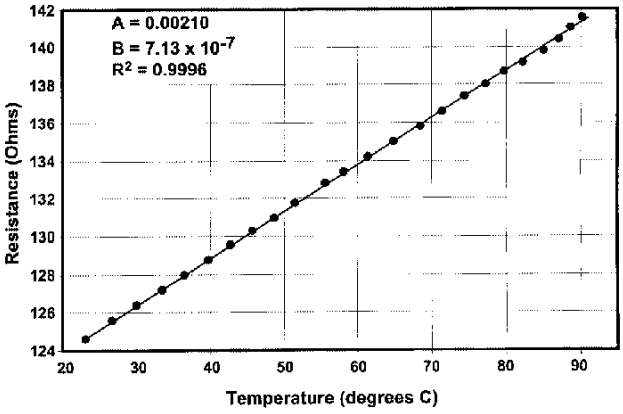

Figure 19. Typical calibration curve of an RTD [35]

5.4. Dimensioning and final configuration combined

The last step was to dimension and connect the output of the DCDC converter so it could supply the amplifier which conforms the instrumentation.

Because part of the voltage supplied by the DCDC converter is stored in the capacitor associated, as the capacitor value increases, the voltage stored decreases and thus, the stability of the output increases because the less voltage is stored the more voltage can be supplied. In this sense, to test the limit, different values for the capacitor were considered starting from lower values and increasing them.

Hence, the final configuration was the following:

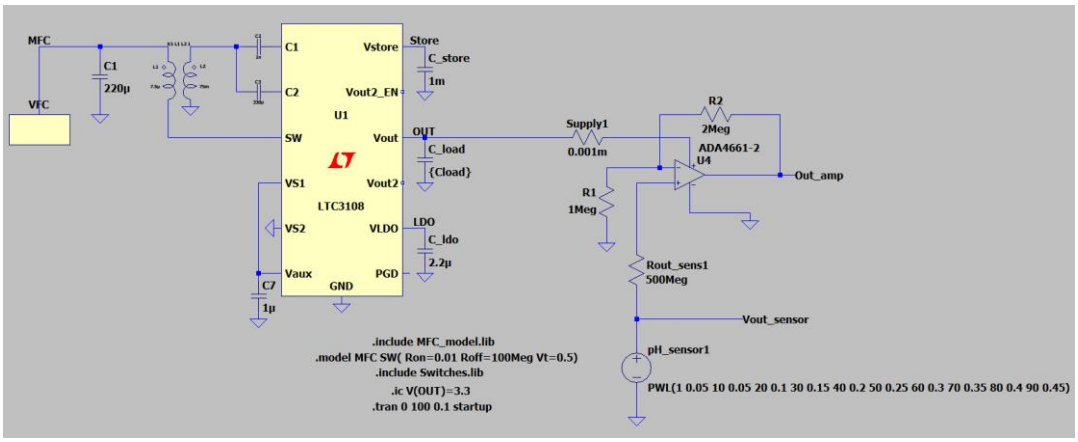

Figure 20. Final configuration of the system

6. Results and discussion

For each of the parts, the simulations were performed using different spice directives depending on which was the variable of interest.

6.1. MFC simulation

For the MFC simulation, various *transient* analysis were performed with a duration of 6 milliseconds.

6.1.1. Single MFC configuration

The first result obtained was the one of the voltages and the current obtained with respect to time.

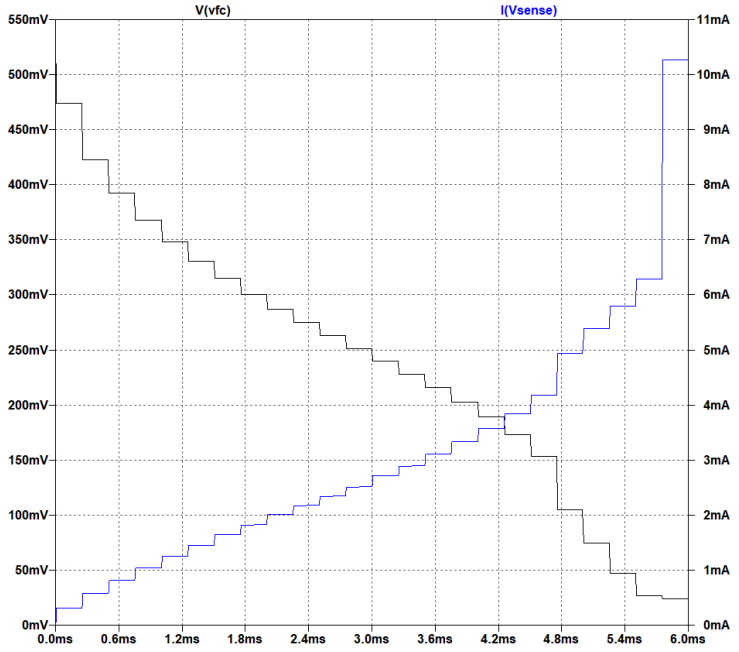

Figure 21. Voltage and Current in the fuel cell with respect to time

The voltage obtained sits in a range between the 546 mV in open circuit and the minimum value of 23 mV. In terms of current, the maximum value corresponds to 10.3 mA.

Then, the polarization curve was plotted placing the current in the x-axis. Below, the first figure corresponds to the reference used while the second one is the experimental result obtained. The x-axis of the experimental one has been limited to 6.3 mA as the variation of voltage for the ranges 6-10 mA was neglectable.

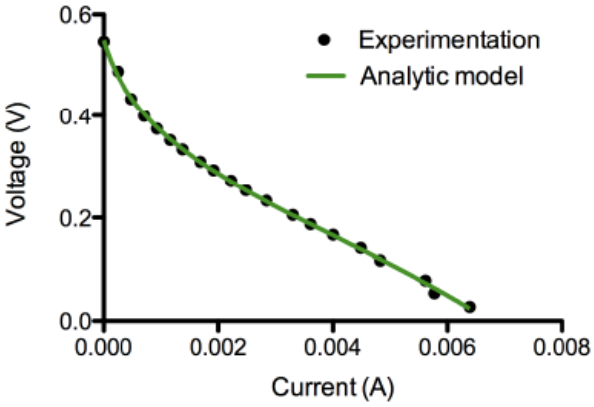

Figure 22. Reference polarization curve [28]

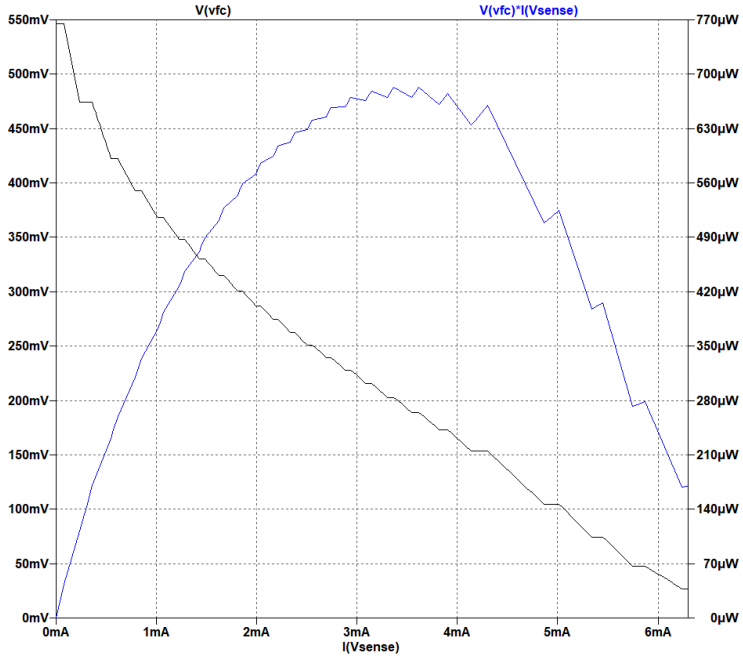

Figure 23. Experimental polarization curve

When comparing both, it can be concluded that the simulation has been performed correctly and the different working points have been captured. As it can be observed, the voltage decreases when the current increases imitating the losses experimented in a real cell due to transportation of the reactants, metabolism and activation and conduction between the different elements, among others.

Also, the power delivered by the MFC, which can be seen in blue, has two extreme points (open-circuit voltage and short-circuit voltage) and between them, the maximum power point (MPP) is found. In this case, the MPP was of 682 µW.

In reference to the instantaneous power, which is interesting to dimension the electronics that can be supplied, it is represented in curve depicted in figure 24.

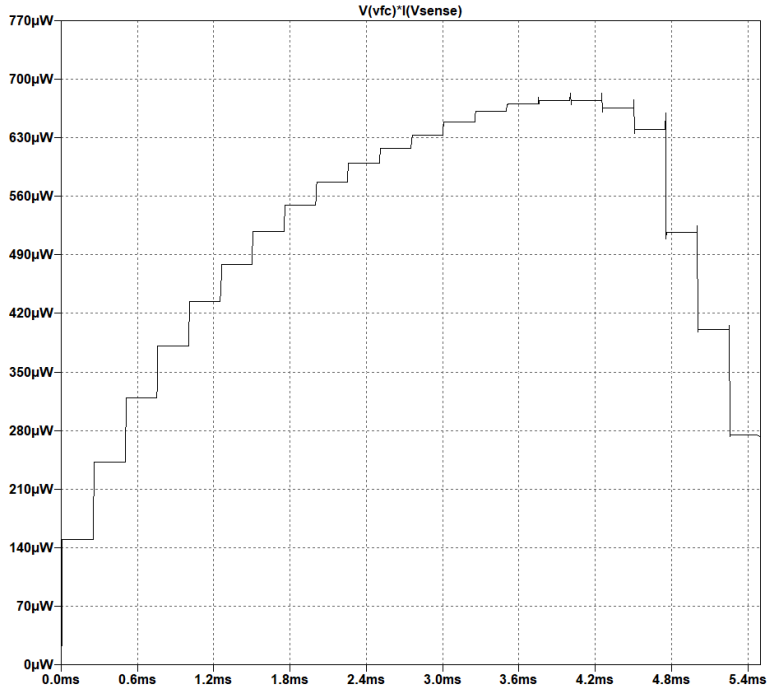

Figure 24. Instantaneous power obtained with a single cell configuration

The maximum value obtained was of 680 µW with an average value of 514 µW and an energy value associated of 2.8309µJ.

The values obtained represent the voltage and current ideal characteristics of the fuel cells but do not accurately represent the real performance of the fuel cell.

6.1.2. Stacked fuel cells

The following figures represent the results obtained for the different configurations simulated. For each option, the corresponding axis were adjusted.

6.1.2.1. Series configuration

The polarization curve obtained was equal to the one for the single case but with the voltage doubled for the same values of intensity.

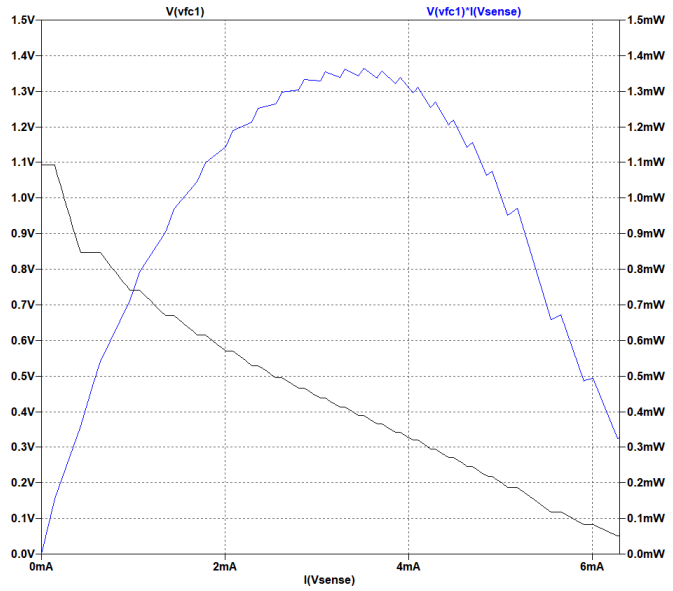

Figure 25. Polarization curve and power curve for 2 stacked cells in series

As it was expected, the voltage was multiplied by two, while the current remained the same. In this way, the OC voltage resulted in 1.09 V. In terms of the power, the MPP was of 1.362 mW.

The average power supplied was of 1.0743 mW while the integral, and thus the energy associated, was of 5.8013 µJ.

As the results for larger number of fuel cells stacked increase proportionally to the number of fuel cells these curves were not included and rather a summary table can be seen below:

Number of fuel cells stacked	V_{OC} (V)	I_{SC} (mA)	MPP (mW)	Average P_i (mW)	Energy (µJ)
1	0.546	6.3	0.682	0.514	2.8309
2	1.09	6.3	1.362	1.074	5.8013
3	1.64	6.3	2.025	1.557	8.4099
4	2.18	6.3	2.700	1.980	10.693

Table 3. Summary of the electrical outputs of different series stacked options

6.1.2.2. Parallel configuration

For this case, the polarization curve obtained was the following:

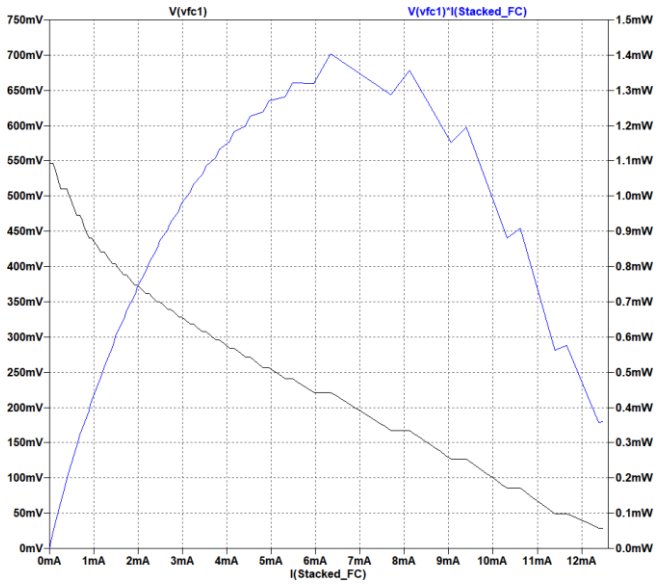

Figure 26. Polarization curve and power curve for 2 stacked cells in parallel

Number of fuel cells stacked	V_{OC} (V)	I_{SC} (mA)	MPP (mW)	Average P_i (mW)	Energy (µJ)
1	0.546	6.3	0.682	0.514	2.8309
2	0.546	12.6	1.335	0.860	5.1609
3	0.546	18.9	2.022	1.167	7.0004
4	0.546	25.2	2.813	1.431	8.5835

Table 4. Summary of the electrical outputs of different parallel stacked options

6.2. Power Management Unit

Having the starting point with a load of 1 GΩ, the characterization of the different outputs was examined.

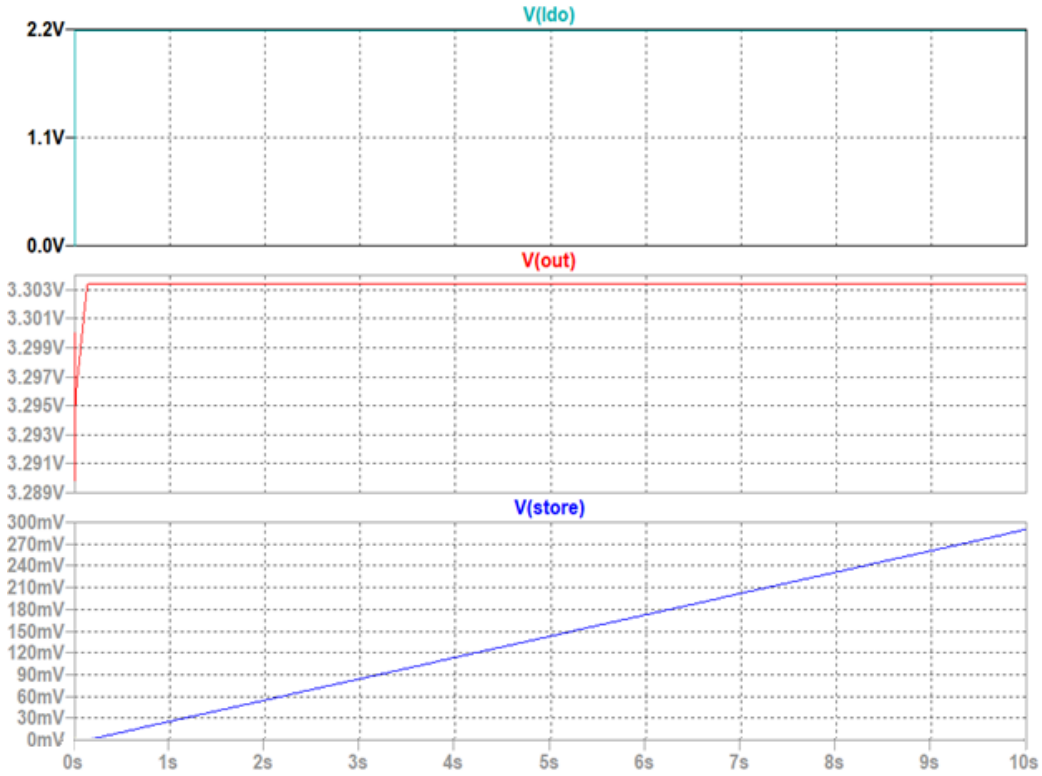

Figure 27. Different output levels of the DCDC converter

The voltage at the *LDO* node, seen in the upper part, has a value of 2.2 V and indicates if the DCDC is starting to work or not. It was observed that its value stayed stable throughout the whole operation.

The output voltage can be seen in the *OUT* node and the load is placed here. Because of the characteristics of the DCDC converter used, this value here stays regulated and stable with a value of 3.3 V.

Finally, the *Store* node which can be seen in blue corresponds to the stored voltage in the capacitor associated to this node. This node is responsible of storing energy, for that reason, at the start of the operation the value has a value of zero and increases with time continuously.

Because both the resistor and the capacitor placed in the *OUT* node influence the behaviour of the system, their effects on the output were examined.

To do so, first, the value of the load resistance was varied between 1kΩ and 500MΩ in different batches in order to assess the current drawn by the load resistance. The power in the load node was also examined as it will be interesting to know the electronics that will be powered after.

Rload (Ω)	Order of magnitude I_{LOAD}	I_{LOAD}	Order of magnitude P_{LOAD}	P_{LOAD}
100K	µA	33	µW	108
200K	µA	16.5	µW	54
300K	µA	11	µW	36
400K	µA	8	µW	27
500K	µA	6.5	µW	22.5
1M	µA	3.3	fW	0.0027
200M	nA	16.5	fW	0.0021
400M	nA	8.3	fW	0.0011

Table 5. Values of current and power for each resistance

It was found that, for values of resistance equal or above 100 kΩ, the power supplied was almost 0 W and were not considerably affected by the value of the capacitor. However, when values of resistance of 10 kΩ were assessed, it was found that, as the capacitance value increased, the decay of the power supplied occurred at lower, more stable rates.

Then, the value of the load was changed in a range between 0.47 mF and 470 mF and the outputs were analyzed for given value of the resistance. In terms of the dependance of the power supplied depending on the capacitor used, the results were the following. For the initial value of the capacitor which was 0.47 mF:

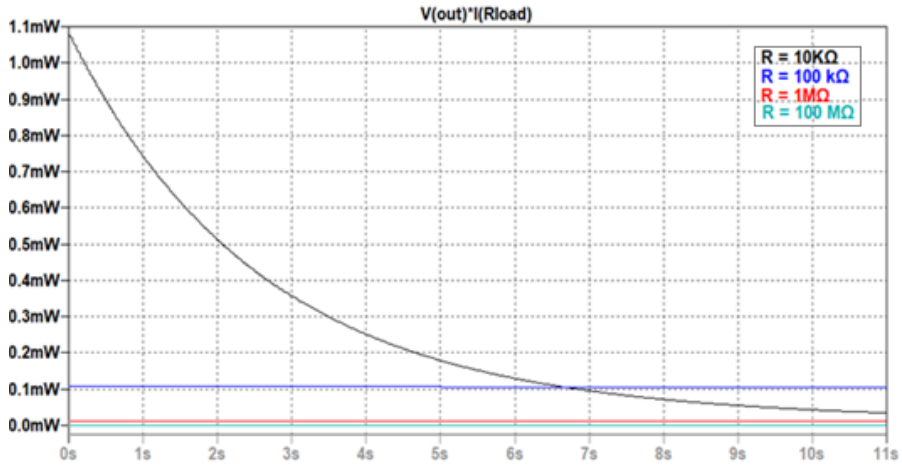

Figure 28. Dependance of the power on the resistance and capacitor value (C = 0.47 mF)

As it was expected, for the low-value resistance, the value decays rapidly in a exponential type of curve.

Conversely, for a capacitor value of 470 mF:

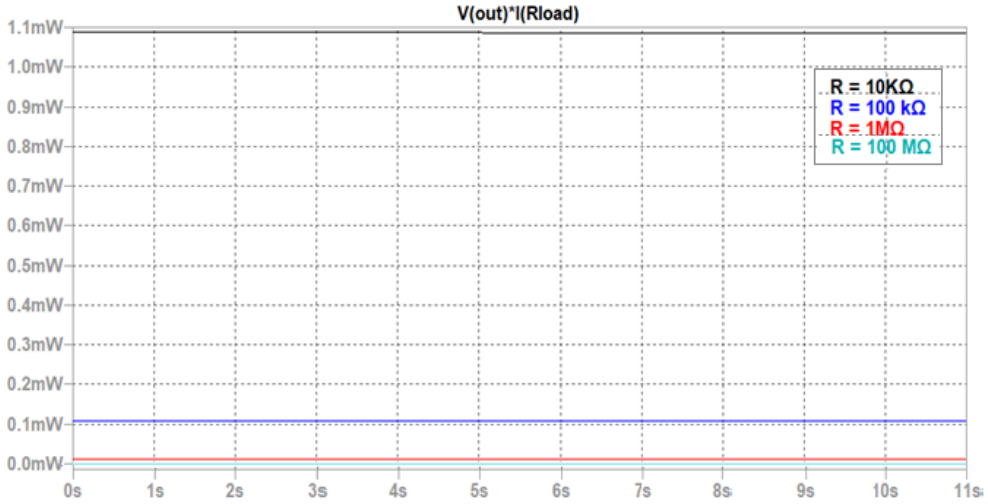

Figure 29. Dependance of the power on the resistance and capacitor value (C = 470 mF)

It can be seen how for this value of the capacitor, the power remains much more stable and thus it is confirmed that for higher values of the capacitor the system will be able to maintain itself running for longer.

Finally, the energy stored in the *STORE* node was also assessed without adding a load in the *OUT* node:

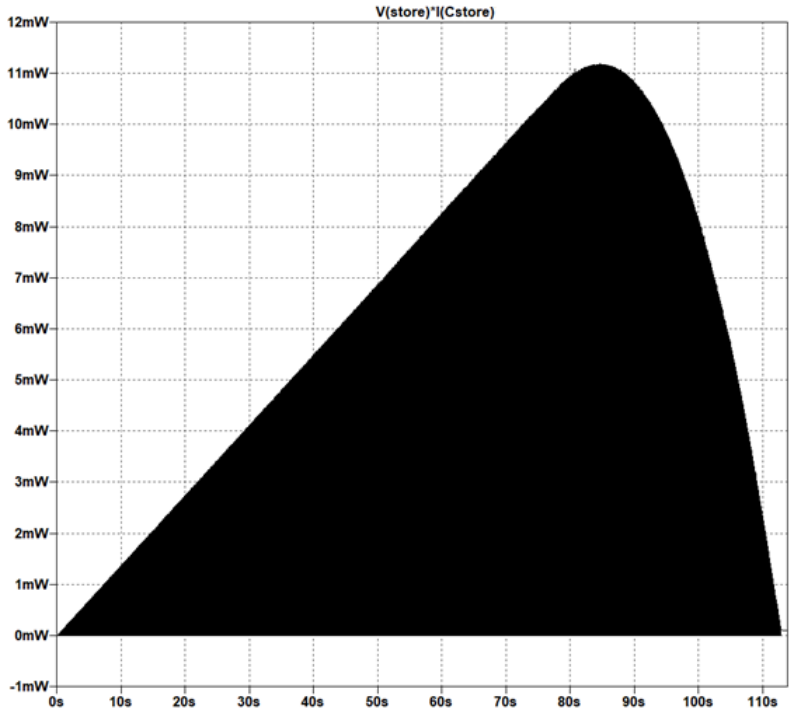

Figure 30. Power curve in the store node

The power was assessed integrating the curve and the value obtained was of 5.93 mJ.

6.3. Instrumentation

6.3.1. pH sensor

As a first step of this study, because it was necessary to assess the power drawn by the instrumentation in order to dimension the previous parameters, the power associated to the *Vdd* input was obtained.

The levels of voltage and current drawn by the amplifier was also displayed.

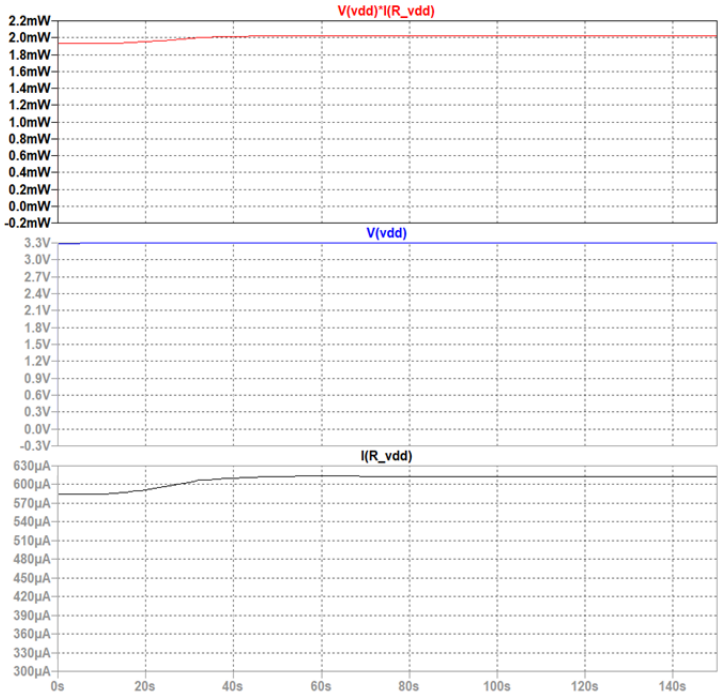

Figure 31. Power, voltage and current needed for the pH sensor

It can be observed that, in terms of power, which can be seen in red, the initial value sits around the 1.9 mW and stays constant until the 40 seconds approximately from where the value increases until reaching a value of 2.0 mW and stays stable for the rest of the time.

The voltage, in blue, stays stable and equal to 3.3V as the voltage source used in this case is an ideal voltameter.

Concerning the current drawn, in black, the starting point was of approximately 585 µA which slightly increases at the 40 seconds reaching a stable value of 2 mW.

Finally, the equivalent resistance of the circuit was also obtained as it would be used to correct the simulations performed with the DCDC converter alone. To do so, the supply voltage was divided by the current drawn following the Ohms law and a resistance of 5.5 kΩ was obtained at first, which then stabilized to a value of 5.4 kΩ.

6.3.2. Temperature modelling for the FC

For the temperature modelling, first, a simulation was performed in which the RTD resistor was combined with the amplifier selected before. In this case, the current applied was of 1 mA with an initial resistance, R0, of 1 kΩ. The gain was also set to a lower value, in this case 1.5. All these decisions were made because if the intensity was in the order of the 10 µA and the resistor in the order of 100 Ω, the value of Vs was in the order of a few tens of mV. Also, there were problems with the output of the sensor, which became 0, for higher temperatures.

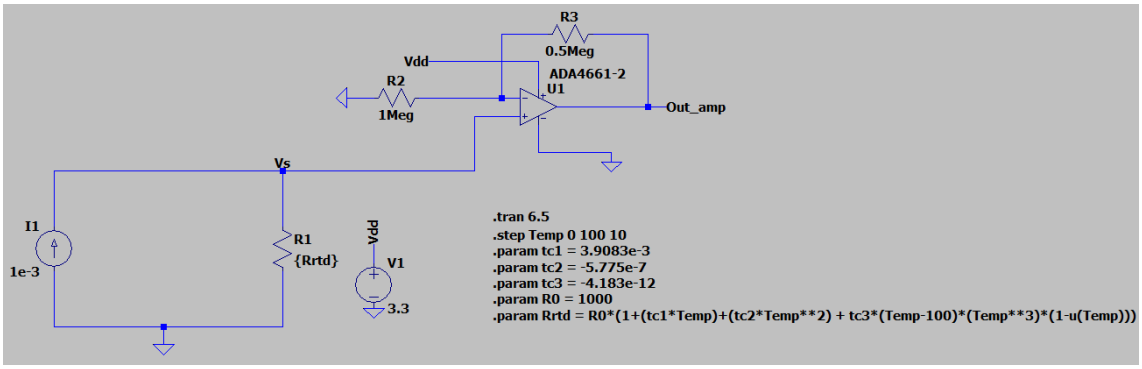

Figure 32. RTD resistor connected to the non-inverting configuration

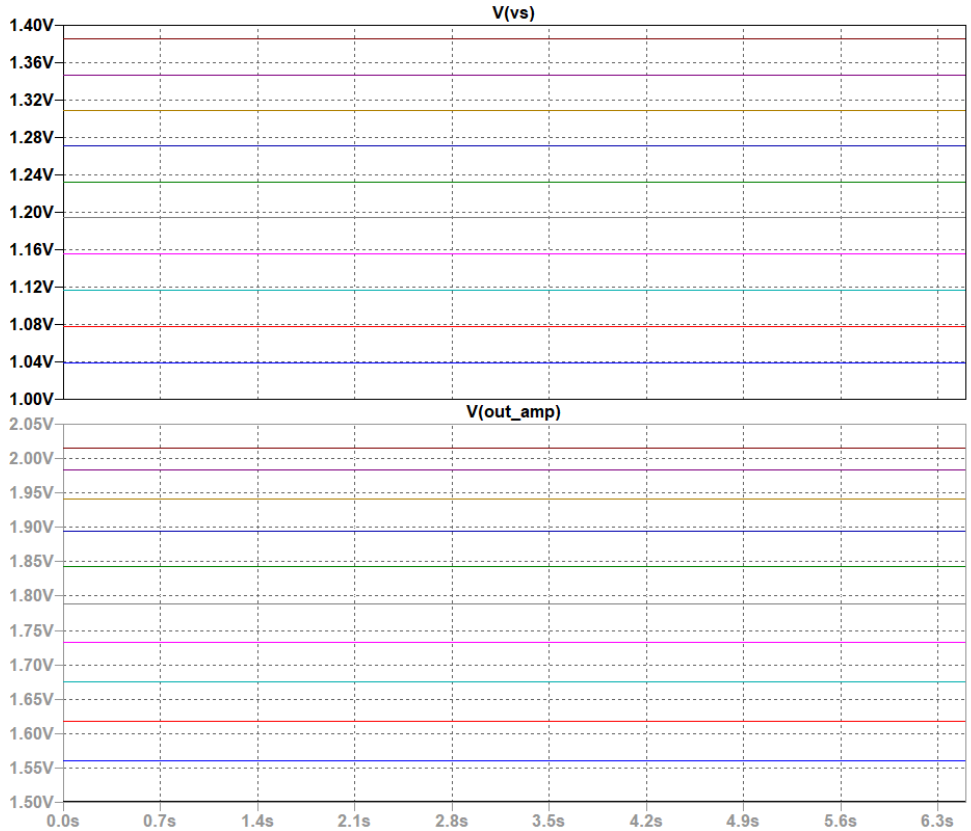

Figure 33. Voltages before and after the op-amp for different temperatures

It can be seen how the different voltages get multiplied by a factor of 1.5 in each case. If these values are represented in a graph in which the x-axis is the temperature and the y-axis the values for each case, the results are the following:

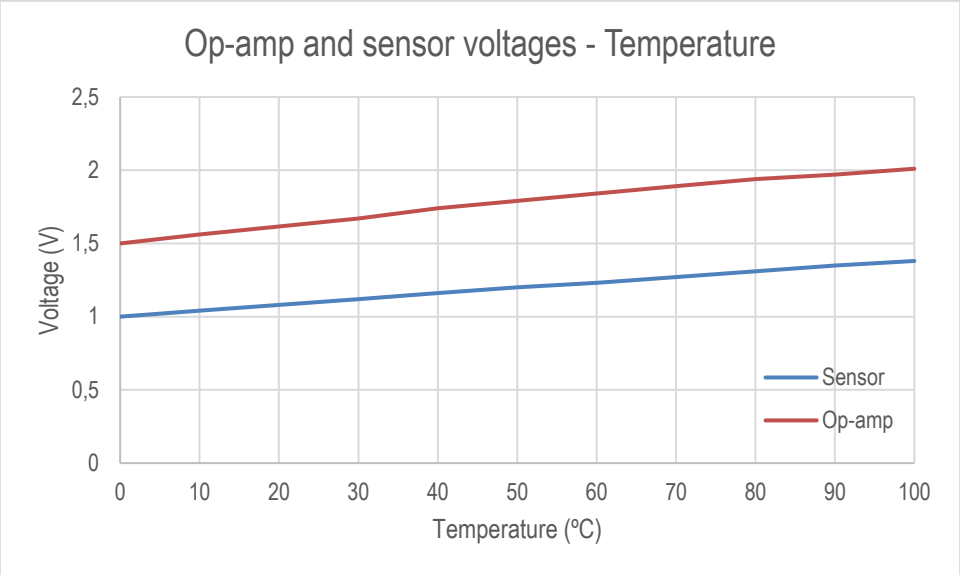

Figure 34. Voltages before and after the op-amp for different temperatures

As it can be seen, the voltages evolution with temperature are almost parallel, starting from a value of 1 and 1.5 V for the “sensor” and amplifier output voltages, respectively.

Finally, a simulation was performed in which the RTD was applied directly to the resistor conforming the fuel cell. In this way, the temperature variations are directly sensed by the fuel cell.

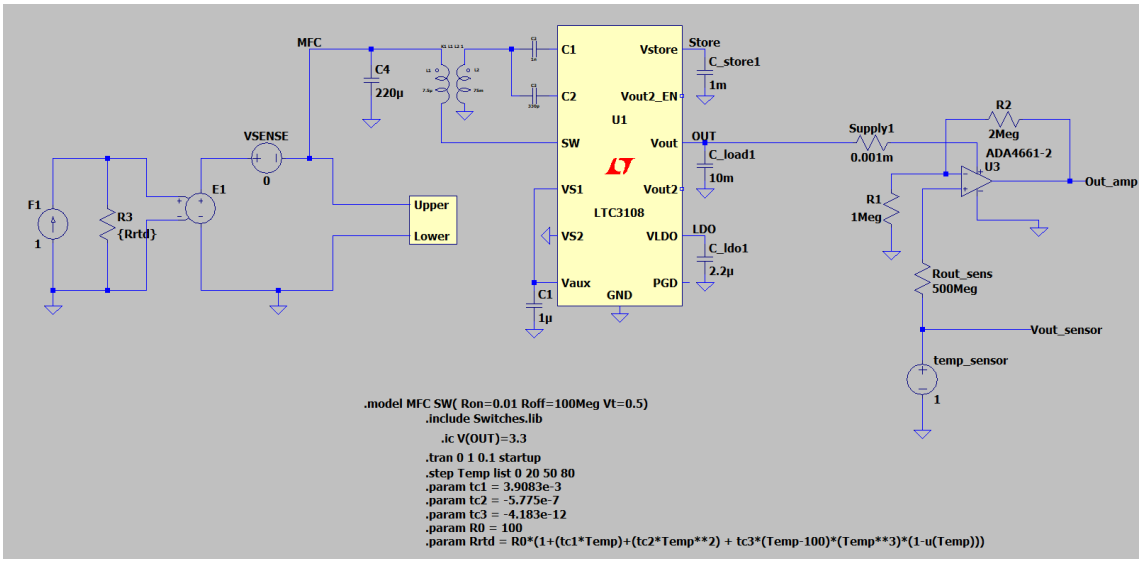

Figure 35. Schematic used for the application of the RTD concept with the FC

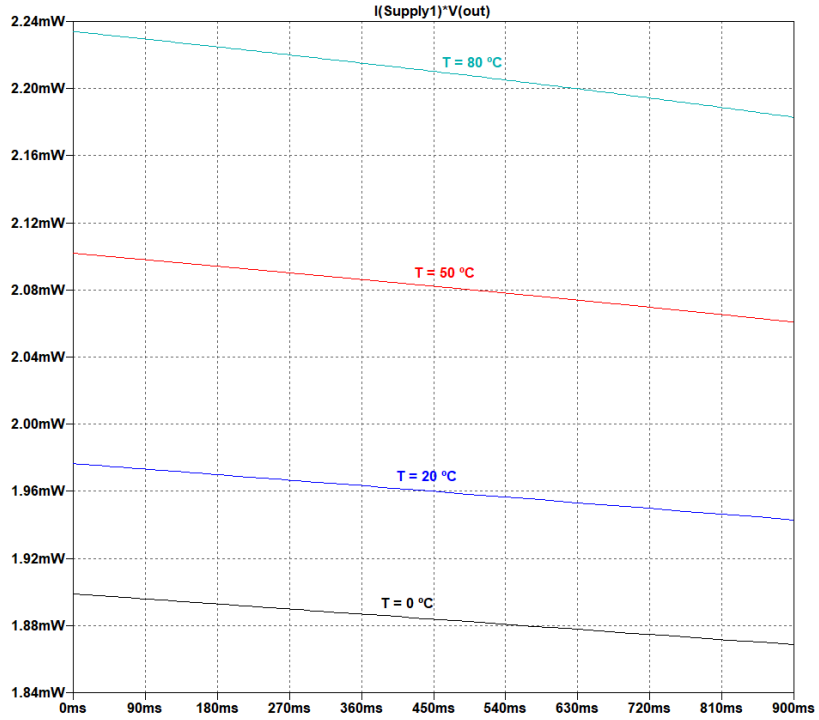

Figure 36. Transient dependance of the power on the temperature (RTD)

It can be noted how the highest power is associated with higher temperatures which makes sense because although the voltage decreases with the increase of temperature the intensity increases and thus by multiplying both terms the result is the increase of the power with the temperature.

6.4. Dimensioning and final configuration combined

Once the whole configuration was brought together, the value of the capacitor was varied. In this case, and because this sensor is the one that has been developed more in depth, only the pH option is considered. Although the schematic has already been presented in the Detail Engineering section, for reading easiness, it has been included below too.

For a starting value of 1 F the system was able to maintain itself running continuously.

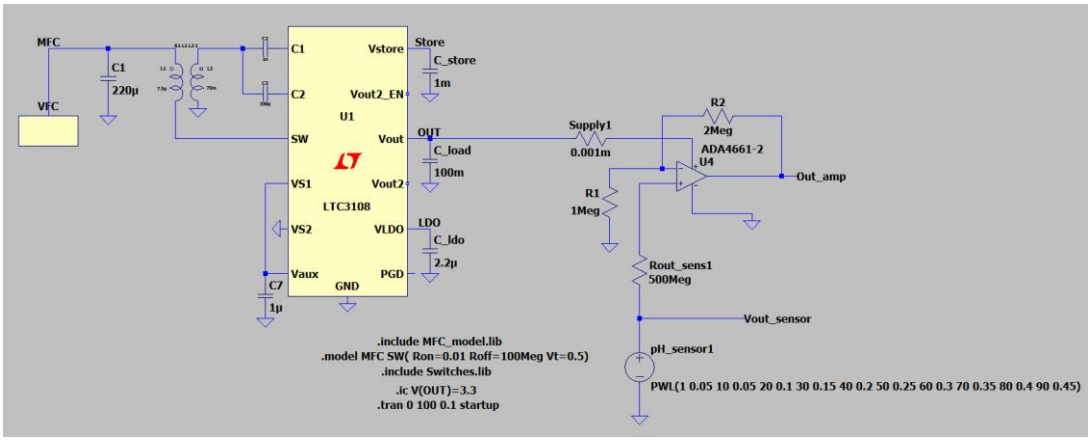

Figure 37. Schematic of the whole configuration (pH case)

When decreasing the value to 100mF, the curve obtained was the following:

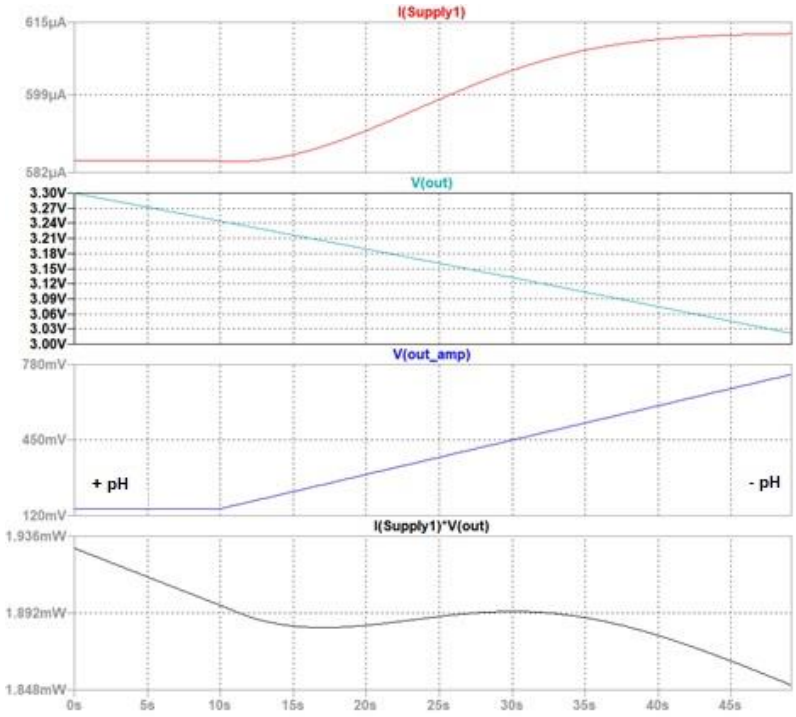

Figure 38. Values of the intensity, voltage and power for the final configuration (Cload = 100mF)

It was observed that, for the initial times, the power decayed linearly until reaching a value of 1.888 mW at approximately 14 seconds. Then, the value started increasing slowly. When observing the current value, it is observed that for times up to the 14 seconds mark, the value is stable and equal to 585 µA. Because the value is stable while the voltage decreases, the power decreases.

From the 14 seconds mark, the current increases slowly until reaching the 610 µA approximately.

However, although the current increases slightly, because once having arrived to the 610 µA mark the value stays constant but the voltage continues decreasing slowly, the power will continue decaying slowly. One strategy would be to use higher values of the capacitor, for instance 470 mF to ensure the functioning for longer.

7. Technical viability

Below, the technical aspects that affect the viability of the project are exposed and analyzed.

Because of the COVID-19 pandemic and the restriction of access to the university laboratories, a completely computer-based alternative had to be selected as defined by the project coordinator. Due to this, no physical facilities have been needed.

However, because the practical part of the project is based on the performance of simulations some software have been used.

First of all, for the analysis of the polarization curve reference and in order to take numerical data points from the graph, the tool ***WebPlotDigitizer*** has been used. This software can be used directly via their website or can also be downloaded completely free of charge.

Then, to perform the simulations, the software **LTSpice** has been used. **LTSpice** is a SPICE simulation software developed by AnalogDevices (AD), previously Linear Technologies, which includes macromodels for the majority of components designed by AD. The program can be downloaded from the original website for either Windows or Mac for free.

Finally, for the development of the written memory and the preparation, **Excel**, **Word** and **PowerPoint** are needed. These programs allow for the creation of spreadsheets, documents and presentations in a visually pleasant way. Microsoft Office package includes all three programs.

In order to assess the technical previability, below, the SWOT (Strengths, Weaknesses, Opportunities and Threats) analysis of the proposed solution is presented:

Some profit can be taken from the weaknesses because, although the range of conditions assessed is low, this can lead to a more in-depth analysis of these conditions. To reduce the threats' impact, a good electronic configuration should be designed.

Also, taking advantage of the strengths, the availability of previous work performed in the same lab offers the possibility of seeking for help.

Strengths	Weaknesses
Easy to replicate and with possibility of moving to different scenarios Cheap and simple methods Good approximation to the values Work in the field already developed by groups in the lab	No previous experience in the field of MFCs Low range of conditions assessed Lack of knowledge to analyze thoroughly all the results
Opportunities	**Threats**
Need for the study of alternative sources of power supply Increased interest in green energy Increased awareness of the effects of environment in human's health	Obtention of unrealistic results due to not considering dynamic characteristics Existence of other projects in the field with more advanced techniques

Table 6. SWOT analysis of the project

8. Forecast schedule

In order to make sure that the project was feasible, it was necessary to perform a time planification and distribution. To do so, in the following pages, an overview of the timing of the project is displayed including the tasks definition and times, the PERT diagram showing the critical path and the GANTT diagram with an overview of the times dedicated to each task of the EDT.

8.1. Task definitions and times

First of all, the tasks that would have to be developed in order to complete the project had to be defined. It was important to also specify the time that it would be needed for the development of said tasks.

The project has been designed with a duration of 300h approximately which will be distributed between the first week of May 2020 and the 21st of June 2021 which is a total of approximately 13 months.

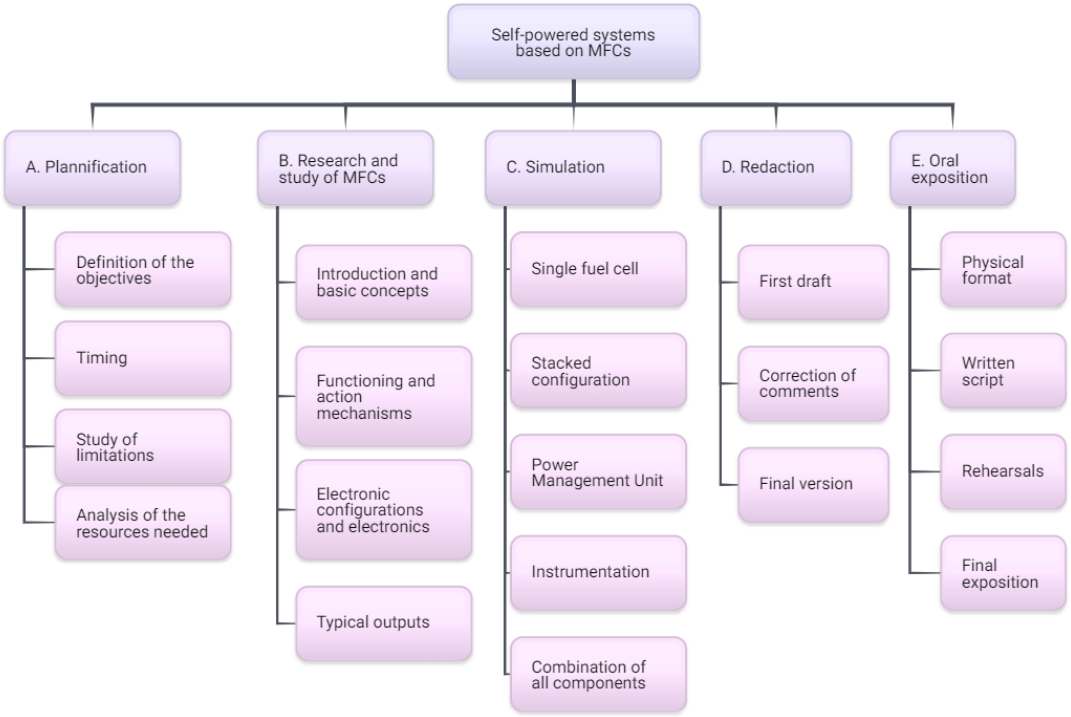

Figure 39. Work Breakdown Structure of the project

As it can be seen, the work is divided in mainly three big parts: planification and research (blocks A and B), experimental part (block C) and exposition of the work performed (blocks D and E).

A. PLANIFICATION.

This is the first part of the project and one of the most important as it includes all the steps involved in defining what is going to be done, how, what could go wrong and what it is needed to carry out the project. It allows the prediction of possible later complications and also allows preparing for solving those issues.

A.1. Definition of the objectives. To know which will be the approach of the project it is important to define exactly what is going to be done and which aspects are included in the span and scope.

A.2. Timing. The time available for the development of the work has to be computed and a reasonable division of time for the different parts has to be performed. It is important as timing of each part should be proportional to the amount of work, realistic considering the hours available to dedicate to the project and also provide a margin in case some unforeseen would occur.

A.3. Study of limitations. In order to reduce the unforeseen events as much as possible, the limitations that could produce problems have to be analyzed and measures have to be studied to minimize their effect as much as possible.

A.4. Analysis of the resources needed. The final planification task is to predict which are the resources that will be needed in order to fulfill the objectives taking into account possible limitations due to covid-19.

B. RESEARCH AND STUDY OF MFCs.

This part corresponds to all the technical information that needs to be collected to have the knowledge necessary to be able to do and fully understand the simulations later performed.
It is necessary not only to research microbial fuel cells themselves but also the electronics that will be fed by them.

B.1. Introduction and basic concepts. As a first step, the definition of what a fuel cell is and which are the concepts associated with it must be researched. The different types of fuel cells have to also be briefly studied to have an overview of the subject.

B.2. Functioning and action mechanisms. Secondly, the MFC has to be studied more in depth and the electrical mechanisms by which it generates energy have to be analyzed in terms of reactions, time-dependance, etc.

B.3. Electric configurations and components. The different options in terms of configurations of the fuel cells have to be studied including the different stacking options. In addition, for the rest of the components that will be used such as DCDC converters and amplifiers the datasheets need to be obtained.

B.4. Typical outputs. In order to understand if the simulations have been performed correctly, references have to be obtained to know if the ranges of values obtained via simulation are reasonable.

C. SIMULATION.

This part consists on simulating the different electric configurations studied previously and applying electric signal to obtain the corresponding curves and analyze the performance of the system. It includes not only the individual analysis of each of the parts but also the combination of all of them and the assessment of the system as a whole.

C.1. Simulation of a single fuel cell. As a first approximation, the simulation of a single fuel cell will be carried out to know the ranges of values that can be obtained. The proposal of a model is necessary and also the obtention of different curves that could explain its characteristics.

C.2. Study of the effects of stacking. In order to study the effects of stacking different fuel cells, simulations with series and parallel configurations will be performed and the range of values obtained will be analyzed considering previous knowledge on this type of configurations.

C.3. Power Management Unit study. The PMU needed to conditionate the signal from the MFC will be simulated using different values for the different components associated such as resistors or capacitors. Variations in these values need to be carried out in order to obtain outputs which will be analyzed.

C.4. Instrumentation analysis. The instrumentation, both the pH and the temperature sensors, that will be supplied with the DCDC converter has to be also assessed in terms of electrical needs that will be provided later.

C.5. Analysis of the results overall. As a final step, the total circuit with all the components connected will be analyzed electrically to check for the stability and the ability of the system to maintain itself running.

D. REDACTION.

This task block includes the redaction of this written memory including all the different parts that compose it. It also includes the discussion of the results obtained in the experimental part.

D.1. First draft. Firstly, an initial draft of the memory will be written with an idea of what the project will be.

D.2. Correction of the commentaries of the tutor. The first version will be sent to the tutor and with the feedback provided, modifications will be made into the original version to improve some of the parts.

D.3. Final version. A final revision will be done and it will be checked that there are no structural errors or related.

E. ORAL EXPOSITION.

Preparation and execution of the oral part of the project.

E.1. Physical format. The PowerPoint in which the project will be presented to the jury will be prepared with the different parts that compose the study.

E.2. Written script. A general guideline will be written in order to practice the oral presentation.

E.3. Rehearsals. The presentation will be practiced several times to perfect the performance of it.

E.4. Final exposition. In the final day of the project, the exposition will have to be done in front of the jury and also some questions will be answered.

8.2. GANTT diagram

For the GANTT diagram, the following tasks identifications have been used. The diagram shows the workflow of the evolution of the project.

Task identification	Definition	Duration in weeks	Duration in hours	Dates
A	Planification	6	27	May 1st – June 15th, 2020
B	Research and study of MFCs	20	83	June 16th - November 1st 2020
C	Simulation	33	117	September 16th, 2020 – May 1st, 2021
D	Redaction	12	50	March 22nd – June 13th, 2021
E	Oral exposition	6	16	May 15th – June 21st, 2021
		77	293	

Table 7. Times and dates associated with each task

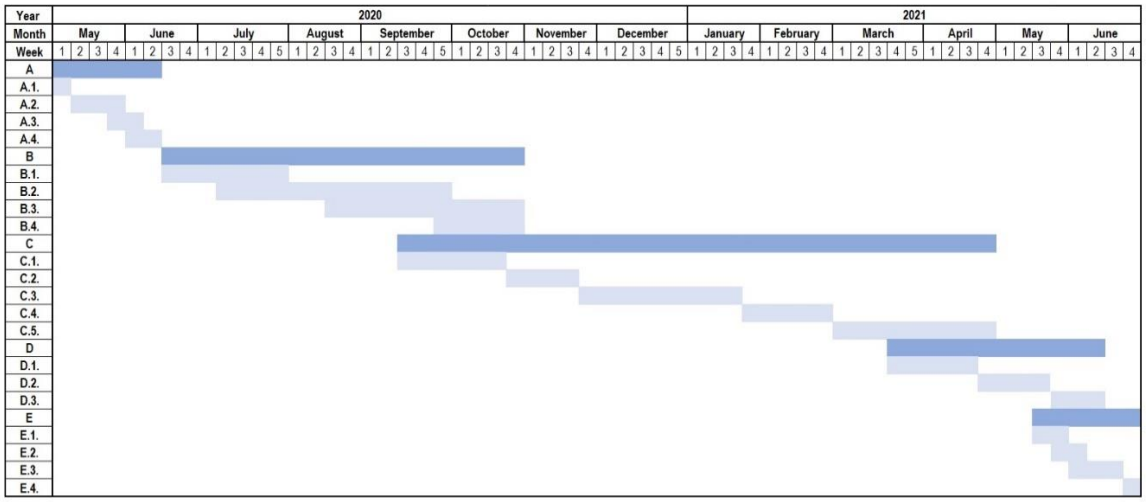

Figure 40. GANTT diagram

9. Conclusions and future lines

To conclude, regarding the objectives of this project, the planification and development have been carried out taking into account the time available for the processes. The procedures have been documented during all the development and with that information, this memory has been written. In terms of the realistic goals setting, the system's objectives have also been achieved so it can be concluded that they were realistic.

Considering the system itself, an extensive study on MFCs has been performed and several electrical modeling have been performed. In addition, significant results, which have made it possible to study the characteristics of the electronic system, have been obtained. During this project, the correct dimensioning of an instrumentation as well as the management of the energy produced by a MFC have been assessed too.

The use of MFCs as energy supply is an incipient topic but the development of new technologies which are able to extract the maximum energy possible can suppose a great future for this field. The increasing scarcity of traditional fuels will surely suppose the further development of these and other systems.

The work performed in this study, a part of being of great utility for consolidating previous knowledge, has also served as an opportunity to understand how a system can be dimensioned and what is the potential of alternative forms of energy.

In terms of future work, more simulations could be performed to exactly determine the value of the capacitor which makes it possible for the system to function properly as the value of 470 mF is only an estimation based on the results obtained.
As for the instrumentation, the models are quite simple and could be improved, especially the temperature one, for which only an initial approximation has been carried out. It would also be interesting to acquire a commercial fuel cell and perform the tests in the laboratory, comparing the experimental results with the simulations performed.
Finally, if the system would have to be created, the legal aspects should be considering as bacteria handling would be involved.

10. References

[1] *Constitution*. Who.int. (2021). Retrieved 31 May 2021, from https://www.who.int/about/who-we are/constitution.

[2] Insitute of Medicine. (2001). *Rebuilding the Unity of Health and the Environment: A New Vision of Environmental Health for the 21st Century*. National Academies Press. https://doi.org/10.17226/10044</p

[3] Rai, P., Lee, S., Zhang, M., Tsang, Y., & Kim, K. (2019). Heavy metals in food crops: Health risks, fate, mechanisms, and management. *Environment International*, *125*, 365-385. https://doi.org/10.1016/j.envint.2019.01.067

[4] *What is pH? | College of Agriculture, Forestry and Life Sciences | Clemson University, South Carolina*. Clemson.edu. (2021). Retrieved from https://www.clemson.edu/extension/food/canning/canning-tips/44what-is-ph.html.

[5] United States Department of Agriculture. (2021). *Soil Quality Kit - Guides for Educators* [Ebook] (p. 1). Retrieved from https://www.nrcs.usda.gov/Internet/FSE_DOCUMENTS/nrcs142p2_053293.pdf.

[6] Oseni, O., Taiwo, A., Ijaola, T., & Yenusa, L. (2016). The Effects of pH On the Levels of Some Heavy Metals in Soil Samples of Five Dumpsites in Abeokuta and its Environs. *International Journal Of Science And Research (IJSR)*, *5*(9). https://doi.org/10.21275/21031604

[7] Blake, L., & Goulding, K. (2002). *Plant And Soil*, *240*(2), 235-251. https://doi.org/10.1023/a:1015731530498

[8] Onwuka, B. (2018). Effects of Soil Temperature on Some Soil Properties and PlantGrowth. *Advances In Plants & Agriculture Research*, *8*(1). https://doi.org/10.15406/apar.2018.08.00288

[9] Hu, Y. (2016). Harvesting the hidden energy for self-powered systems. *2016 IEEE 16Th International Conference On Nanotechnology (IEEE-NANO)*. doi: 10.1109/nano.2016.7751302

[10] Glynne-Jones, P., & White, N. (2001). Self-powered systems: a review of energy sources. *Sensor Review*, *21*(2), 91-98. doi: 10.1108/02602280110388252

[11] Xu, C., Song, Y., Han, M. *et al.* Portable and wearable self-powered systems based on emerging energy harvesting technology. *Microsyst Nanoeng* **7,** 25 (2021). https://doi.org/10.1038/s41378-021-00248-z

[12] Nundrakwang, S., Yingyong, P., & Isarakorn, D. (2020). Energy Harvesting for Self-Powered Systems. *2020 6Th International Conference On Engineering, Applied Sciences And Technology (ICEAST)*. doi: 10.1109/iceast50382.2020.9165350

[13] Logan, B. (2008). *Microbial fuel cells* (pp. 1-11). Wiley-Interscience.

[14] Kumara Behera, B., & Varma, A. (2016). *Microbial Resources for Sustainable Energy*. Springer International Publishing.

[15] Das, D. (2016). *Microbial Fuel Cell*. Spinger International Publisher.

[16] Correon-Bautista, S. (2015). *Power Management Circuits For Energy Harvesting* (Doctor). Texas A&M University.

[17] Pepliński, H. (2019). Integrated Automation System (IAS). *Ship And Mobile Offshore Unit Automation*, 99-122. https://doi.org/10.1016/b978-0-12-818723-4.00011-9

[18] Umaz, R. (2020). A Power Management System for Microbial Fuel Cells With 53.02% Peak End-to-End Efficiency. *IEEE Transactions On Circuits And Systems II: Express Briefs*, *67*(11), 2592-2596. https://doi.org/10.1109/tcsii.2019.2951810

[19] Texas Instruments. (2013). *AN-1852 Designing With pH Electrodes* [Ebook]. Retrieved from https://www.ti.com/lit/an/snoa529a/snoa529a.pdf?ts=1622386055916&ref_url=https%253A%252F%252Fwww.google.com%252F.

[20] *Basics of pH Sensor and pH Value Measurement - Electronics Hub*. Electronics Hub. (2019). Retrieved from https://www.electronicshub.org/basics-of-ph-sensor-and-ph-value-measurement/#How_pH_is_Measured.

[21] Sensor de pH. (2021). Retrieved 7 June 2021, from https://www.mt.com/es/es/home/products/Laboratory_Analytics_Browse/pH-meter/sensor/pH-sensor.html

[22] Ph Meter 0.001ph Resolution. (2021). Retrieved 7 June 2021, from https://www.mrclab.com/ph-meter-0001ph-resolution

[23] Texas Instruments. (2020). *The Engineer's Guide to Temperature Sensing* [Ebook]. Retrieved from https://www.ti.com/lit/eb/slyy161/slyy161.pdf?ts=1622306132888&ref_url=https%253A%252F%252Fwww.ti.com%252Fsensors%252Foverview.html.

[24] Selection Table for Digital Temperature Sensors | Parametric Search | Analog Devices. (2021). Retrieved 7 June 2021, from https://www.analog.com/en/parametricsearch/11020#/

[25] Web of Science. (2021). Retrieved 7 June 2021, from https://apps.webofknowledge.com/UA_GeneralSearch_input.do?product=UA&search_mode=GeneralSearch&SID=F3opdiH9FbUjfXU7b7V&preferencesSaved=

[26] *Microbial Fuel Cell Market Size, Share, Growth | Report, 2027*. Marketresearchfuture.com. (2020). Retrieved from https://www.marketresearchfuture.com/reports/microbial-fuel-cell-market-7194.

[27] *Microbial Fuel Cell Market To Reach USD 19.5 Million By 2026 | Reports And Data*. GlobeNewswire News Room. (2019). Retrieved from http://www.globenewswire.com/en/news-release/2019/07/23/1886558/0/en/Microbial-Fuel-Cell-Market-To-Reach-USD-19-5-Million-By-2026-Reports-And-Data.html.

[28] Degrenne, N. (2012). *Power Management for Microbial Fuel Cells* (Doctorado). Ecole Centrale de Lyon.

[29] Schmitz, T. (2012). Selecting precision op amps for sensor input processing designs. Retrieved 7 June 2021, from https://www.newelectronics.co.uk/electronics-technology/selecting-precision-op-amps-for-sensor-input-processing-designs/44276/

[30] D. Reyta, E., & O. Ochoco, M. pH Sensor Reference Design Enabled for RF Wireless Transmission | Analog Devices. Retrieved 7 June 2021, from https://www.analog.com/en/technical-articles/ph-sensor-reference-design-enabled-for-rf-wireless-transmission.html#

[31] Davis, S. (2021). *Power Management Chapter 13: Energy Harvesting*. Power Electronics. Retrieved from https://www.powerelectronics.com/technologies/power-management/article/21864177/power-management-chapter-13-energy-harvesting.

[32] Operational amplifier basics. (2021). Retrieved 7 June 2021, from https://www.electronics-tutorials.ws/opamp/opamp_1.html

[33] Brand, T. *A Simple Way of Measuring Soil Moisture and pH with Temperature Compensation | Analog Devices*. Analog.com. Retrieved from https://www.analog.com/en/technical-articles/a-simple-way-of-measuring-soil-moisture-and-ph-with-temperature-compensation.html#.

[34] *How sensors work - pH measurement*. Sensorland.com. Retrieved from https://www.sensorland.com/HowPage037.html.

[35] Lagally, E., Emrich, C., & Mathies, R. (2001). Fully integrated PCR-capillary electrophoresis microsystem for DNA analysis. *Lab On A Chip*, *1*(2), 102. doi: 10.1039/b109031n